The 1995–96 decline of R Coronae Borealis: high-resolution optical spectroscopy

N. Kameswara Rao,[1] David L. Lambert,[2] Mark T. Adams,[3] David R. Doss,[3] Guillermo Gonzalez,[4] Artie P. Hatzes,[2] C. Renée James,[2] C. M. Johns-Krull,[5] R. Earle Luck,[6] Gajendra Pandey,[1] Klaus Reinsch,[7] Jocelyn Tomkin[2] and Vincent M. Woolf[2]

[1]*Indian Institute of Astrophysics, Bangalore 560034, India*
[2]*Department of Astronomy, University of Texas, Austin, TX 78712-1083, USA*
[3]*McDonald Observatory, Fort Davis, TX 79734-1337, USA*
[4]*Department of Astronomy, University of Washington, PO Box 351589, Seattle, WA 98195-1580, USA*
[5]*Space Science Laboratories, University of California, Berkeley, CA 94720-7450, USA*
[6]*Department of Astronomy, Case Western Reserve University, Cleveland, OH 44106-7215, USA*
[7]*Universitäts-Sternwarte, Georg-August Universität, Göttingen, 37083 Germany*

ABSTRACT

A set of high-resolution optical spectra of R CrB acquired before, during and after its 1995–96 decline is discussed. All of the components reported from earlier declines are seen. This novel data set provides new information on these components including several aspects not previously seen in declines of R CrB and other R Coronae Borealis stars. In the latter category is the discovery that the onset of the decline is marked by distortions of absorption lines of high-excitation lines, and quickly followed by emission in these and in low-excitation lines. This 'photospheric trigger' implies that dust causing the decline is formed close to the star. These emission lines fade quickly. After 1995 November 2, low-excitation narrow (FWHM $\sim 12\,\mathrm{km\,s^{-1}}$) emission lines remain. These appear to be a permanent feature, slightly blueshifted from the systemic velocity, and unaffected by the decline except for a late and slight decrease of flux at minimum light. The location of the warm dense gas providing these lines is uncertain. Absorption lines unaffected by overlying sharp emission are greatly broadened, weakened and redshifted at the faintest magnitudes when scattered light from the star is a greater contributor than direct light transmitted through the fresh soot cloud. A few broad lines (FWHM $\simeq 300\,\mathrm{km\,s^{-1}}$) are seen at and near minimum light with approximately constant flux: prominent among these are the He I triplet series, Na I D and [N II] lines. These lines are blueshifted by about $30\,\mathrm{km\,s^{-1}}$ relative to the systemic velocity, with no change in velocity over the several months for which the lines were seen. It is suggested that these lines, especially the He I lines, arise from an accretion disc around an unseen compact companion which may be a low-mass white dwarf. If so, R CrB is similar to the unusual post-asymptotic giant branch star 89 Her.

Key words: accretion, accretion discs – circumstellar matter – stars: individual: R CrB – stars: variables: other.

1 INTRODUCTION

R Coronae Borealis is the prototype of a class of very rare and peculiar supergiant stars with two distinctive primary traits, one photometric and the other spectroscopic. Photometrically, an R Coronae Borealis Star (RCB) is distinct because it declines at unpredictable times by one to several magnitudes as a cloud of carbon soot obscures the stellar photosphere for weeks to months. Spectroscopically, the distinctive signature of an RCB is weak Balmer lines which indicate an atmosphere deficient in hydrogen. Two fundamental questions about RCBs remain unanswered. By what evolutionary paths are some stars with their normal H-rich

atmospheres converted to RCBs with He-rich atmospheres? What are the physical processes that trigger and control development of the unpredictable minima?

In this paper, we discuss spectroscopic observations of the recent deep and prolonged minimum of R CrB, and aim to address the second question. The decline that seems to have begun on or around 1995 October 2 proved to be the deepest and longest decline of recent years. Recovery from the minimum of the decline was slow: even about 1 yr after the onset of the decline, the star was 1 mag below its normal maximum. Throughout this period, we were able to obtain high-resolution optical spectra of the star at quasi-regular intervals.

Our discussion of this novel data set provides new insights into the widely accepted model of RCB declines in which a cloud of carbon soot obscures the star (O'Keefe 1939). There is convincing empirical evidence that the cloud is a localized event and not a spherically symmetric phenomenon. In particular, the infrared excess of the star is largely unchanged during the decline, showing that a large dust cloud exists independently of the new decline and that the largely unobscured star heats this cloud (Feast 1979, 1996). The dusty cloud with a radius of $100\,R_*$ is heated by absorbing about 10 to 20 per cent of the stellar radiation (Forrest, Gillett & Stein 1971, 1972; Rao & Nandy 1986).

How and where the soot condenses has been debated. If dust is to form under equilibrium conditions in a quasi-hydrostatic extension of the stellar atmosphere, the required low temperatures are found only far from the star – say, at 10–20 stellar radii. If regions of the atmosphere are compressed by a shock, the necessary low temperatures can be found for a time much closer to the star – say, at 1–2 stellar radii. Observational and theoretical arguments for the 'far' and 'near' sites of dust formation are reviewed by Clayton (1996; see also Fadeyev 1986). The initial fading of the star has been plausibly interpreted as being due to the lateral growth of a dust cloud.

Earlier accounts of R CrB, RY Sgr and V854 Cen have identified the following principal spectroscopic components that are revealed as an RCB is obscured by soot [see Clayton (1996) for a general review of observational characteristics of RCBs in and out of decline, and of their evolutionary origins].

(i) Sharp emission lines. These lines appear shortly after the onset of a decline and disappear just before the return to maximum light. Alexander et al. (1972), in an extensive study of photographic spectra of RY Sgr, divided these emission lines into two types – E1 and E2. Payne-Gaposchkin (1963) earlier noted the two types. A defining characteristic of E1 lines is that they fade away after about two weeks from the onset of a decline. Membership in E1 has been summarized by the remark that 'this spectrum consists of many lines of neutral and singly ionized metals' (Clayton 1996). To this must be added the comment that the excitation of the E1 spectrum of lines is higher than that of the E2 spectrum. E2 lines are present throughout the decline and are probably permanent features. Prominent in the E2 (and E1) spectrum are lines of ions such as Sc II, Ti II, Fe II, Y II and Ba II, as well as neutral atoms, particularly Fe I. The emission lines are slightly blueshifted with respect to the systemic velocity of the star.

Accounts of these lines were given by Payne-Gaposchkin (1963) and Cottrell, Lawson & Buchhorn (1990) for R CrB, and Alexander et al. (1972) for RY Sgr – see also Rao & Lambert (1993) on V854 Cen and Goswami et al. (1997) on S Aps, both in deep declines.

(ii) Broad permitted and forbidden emission lines. Seen in deep declines, these are much broader than the sharp emission lines. In the case of V854 Cen, for example, the width (FWHM) of the broad lines was about $300\,\mathrm{km\,s^{-1}}$ but the sharp lines were unresolved with a FWHM less than about $20\,\mathrm{km\,s^{-1}}$ (Rao & Lambert 1993).

The first report of forbidden and permitted broad lines in the spectrum of an RCB in decline was Herbig's (1949, 1968) discovery of [O II] 3727 Å and He I 3889 Å in the spectrum of R CrB. Herbig was unable to determine that the linewidths differed from that of the Sc II et al. lines, but attribution of the lines to the group of broad lines now seems evident.

(iii) Photospheric absorption lines. In the early phases of a decline, the sharp emission lines are superimposed on a photospheric spectrum that appears largely unchanged for those lines that do not go into emission. In deep declines, the photospheric spectrum changes. A weakening of the lines noted by Herbig (1949) was confirmed and discussed by Payne-Gaposchkin (1963) and Cottrell et al. (1990) for R CrB. The weakening was attributed to 'veiling', a term implying dilution of the photospheric spectrum by overlying continuous (or line) emission. In an observation of V854 Cen in a deep decline, the continuous spectrum was devoid of lines (Rao & Lambert 1993).

(iv) Shell absorption components. During the recovery to maximum light and into full recovery, blueshifted broad absorption components of the Na I D, and Ca II H and K lines are seen. A velocity shift of $-150\,\mathrm{km\,s^{-1}}$ seems typical. Reports of these lines were given by Payne-Gaposchkin (1963), Rao (1974), Cottrell et al. (1990) and Lambert, Rao & Giridhar (1990) for R CrB, Alexander et al. (1972) and Vanture & Wallerstein (1995) for RY Sgr, and Clayton et al. (1993) and Rao & Lambert (1993) for V854 Cen.
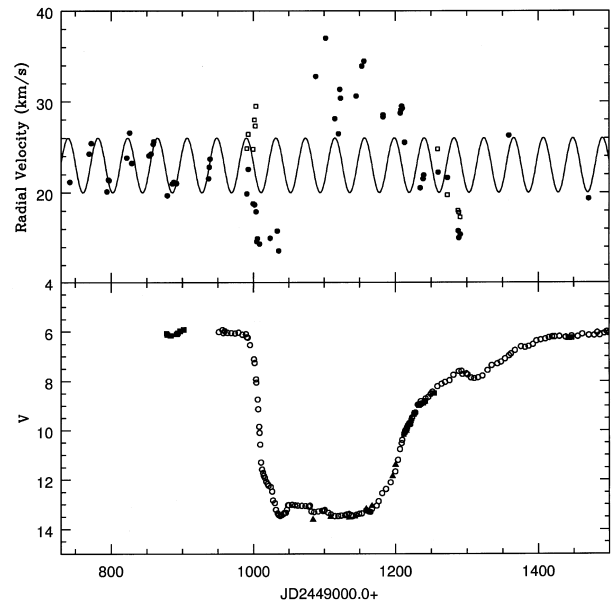
Figure 1. Light curve and photospheric absorption-line radial velocities of R CrB during the 1995–96 decline. The light curve (lower panel) is constructed from visual observations kindly supplied by the American Association of Variable Star Observers (AAVSO) (open circles represent 10-d means) and V magnitudes from Efimov (private communication, filled triangles) and Fernie (private communication, filled squares). Radial velocities (upper panel) are presented for group A (filled circles) and B (open squares) lines (see text).

Table 1. Catalogue of spectra of R CrB.

	Date	JD−2440000.0	Mag[a]	Telescope	Observer[b]	Comments[c]
1995	Jan 24	9742.01	5.9	2.1m	GG	5720–7225
	Feb 20	9768.97	5.9	2.1m	AH	5590–7040
	Feb 23	9771.92	5.9	2.1m	AH	5990–6960
	Mar 17	9793.96	5.9	2.1m	AH	5990–6960
	Mar 19	9796.02	5.9	2.1m	AH	5990–6960
	Mar 20	9797.00	5.9	2.1m	AH	5990–6960
	Apr 14	9821.80	5.9	2.1m	REL/VW	5720–7225
	Apr 18	9825.81	5.9	2.1m	GG	5720–7225
	Apr 21	9828.78	5.9	2.1m	GG	6280–8400
	May 15	9852.85	5.9	2.1m	GG	5760–7300
	May 18	9855.82	5.9	2.7m	JT	
	May 21	9858.80	5.9	2.1m	VW	3930–4275
	May 22	9859.70	5.9	2.1m	VW	3930–4275
	Jun 10	9878.64	5.9	2.1m	GG	5720–7225
	Jun 17	9885.64	5.9	2.7m	JT	
	Jun 19	9887.68	5.9	2.7m	JT	
	Jun 23	9891.69	5.9	2.1m	GG	5760–7230
	Aug 7	9936.61	5.9	2.7m	JT	
	Aug 8	9937.62	5.9	2.7m	JT	
	Aug 9	9938.61	5.9	2.7m	JT	
	Sep 30	9990.62	6.1	2.7m	JT	
	Oct 2	9992.64	6.3	2.7m	JT	
	Oct 7	9997.58	6.8	2.1m	REL	4880–5650
	Oct 8	9998.56	6.9	2.1m	REL	4880–5650
	Oct 9	9999.56	7.0	2.1m	REL	5720–7225
	Oct 11	10001.56	7.1	2.1m	REL	5720–7225
	Oct 12	10002.55	7.3	2.1m	REL	6550–8550
	Oct 13	10003.59	7.7	2.7m	JT	
	Oct 14	10004.56	8.0	2.7m	JT	
	Oct 15	10005.55	8.4	2.7m	JT	
	Oct 16	10006.61	8.8	2.1m	KR	4460–5040
	Oct 17	10007.56	9.6	2.1m	KR	4460–5040
	Oct 18	10008.56	10.1	2.1m	KR	4460–5040
	Oct 18	10008.56	10.1	2.7m	DD	
	Nov 2	10023.54	12.2	2.7m	CRJ	
	Nov 12	10033.54	13.4	2.1m	CJK	5760–7225
	Nov 14	10035.54	13.5	2.1m	CJK	5760–7225
	Nov 15	10036.54	13.5	2.1m	CJK	5760–7225
1996	Jan 5	10088.00	13.57	2.7m	JT	
	Jan 19	10101.98	13.2	2.1m	GG	5570–6780
	Feb 1	10114.96	13.7	2.1m	CJK	5760–7225
	Feb 6	10119.99	13.50	2.7m	JT	
	Feb 8	10122.01	13.6	2.7m	JT	
	Feb 9	10123.01	13.6	2.7m	JT	
	Mar 2	10144.95	13.45	2.7m	SLH/DLL	
	Mar 10	10152.99	13.5	2.1m	AH	5020–5910
	Mar 13	10155.90	13.4	2.1m	AH	5020–5910
	Apr 9	10182.75	12.47	2.1m	GG	5510–6790
	May 3	10206.90	10.8	2.7m	DLL	
	May 4	10207.88	10.7	2.7m	DLL	
	May 5	10208.85	10.40	2.7m	DLL	
	May 6	10209.85	10.5	2.7m	DLL	
	May 9	10212.82	10.07	2.1m	GG	5720–7220
	May 31	10234.78	8.93	2.1m	CRJ	5720–7300
	Jun 4	10238.77	8.88	2.1m	AH	5840–7360
	Jun 5	10239.63	8.85	2.1m	AH	5990–7820
	Jun 25	10259.72	8.1	2.1m	GG	5480–6780
	Jul 8	10272.73	8.0	2.7m	CRJ	
	Jul 23	10287.65	7.4	2.7m	DLL	
	Jul 24	10288.61	7.5	2.7m	DLL	
	Jul 26	10290.64	7.5	2.7m	DLL	
	Oct 2	10358.55	7.0	2.7m	DLL	5880–5902

[a] Visual magnitude from AAVSO. *V* (given to second decimal) from Fernie (private communication) and Efimov (private communication).
[b] Observers: DD = David Doss, DLL = David L. Lambert, GG = Guillermo Gonzalez, AH = Artie Hatzes, CRJ = C. Renée James, CJK = Chris Johns-Krull, REL = R. Earle Luck, SLH = Suzanne Hawley, KR = Klaus Reinsch, JT = Jocelyn Tomkin, VW = Vincent Woolf.
[c] This gives wavelength interval in Å for the 2.1-m spectra.

In this study of the 1995–96 deep decline of R CrB, we discuss these spectroscopic components with an emphasis on novel results. With our temporal and spectral coverage, new detailed information is provided on all of the previously seen principal components. Since the decline was preceded by a long interval in which R CrB was at or near maximum light, it is most likely that all of the spectroscopic changes are associated with the decline and none is a residual effect of earlier declines. Following a description of the sequence of spectra acquired from 1995 to 1996, discussion is arranged chronologically beginning with descriptive remarks on the spectrum of the star prior to the decline, continuing with spectroscopic changes associated with the onset of the decline, and concluding with remarks on the several components present in the spectrum from about mid-decline through the extended period of minimum light and into the recovery phase. These descriptions are followed by interpretative remarks on a model of R CrB, including a suggestion that this star may be a spectroscopic binary.

2 OBSERVATIONS

Spectra were obtained at the W. J. McDonald Observatory with either the 2.7-m or the 2.1-m reflector. The light curve of R CrB through the decline is shown in the lower panel of Fig. 1 where the sources of the photometry are identified. The upper panel gives radial velocity measurements and the predicted velocity variation owing to pulsation (see below). The measurements serve to indicate the relation between our observations and the phase of the decline – see also Table 1.

At the 2.7-m telescope, the coudé cross-dispersed echelle spectrograph (Tull et al. 1995) was used with the camera that gives a maximum (two-pixel) resolving power of $R = \lambda/\Delta\lambda = 60\,000$. The detector was a Tektronix 2048×2048 CCD. The recorded spectrum ran from about 3800 to 10 000 Å, but spectral coverage was incomplete longward of about 5500 Å. A Th–Ar hollow cathode lamp providing a wavelength calibration was observed either just prior to or just after exposures of R CrB. The pixel-to-pixel variation of the CCD was removed using observations of a lamp providing a continuous spectrum. Typical exposure times for R CrB in decline were 30 min, with multiple exposures co-added as necessary to improve the signal-to-noise ratio of the final spectrum. Occasionally, an early-type rapidly rotating star was observed to provide a template of the telluric absorption lines.

The Sandiford Cassegrain echelle spectrometer (McCarthy et al. 1993) was used at the 2.1-m telescope. These spectra have a resolving power also of approximately $R = 60\,000$. Although the wavelength coverage at a single exposure (see Table 1) is less extensive than at the 2.7-m, orders of the echelle are completely recorded for wavelengths shorter than about 7500 Å. Calibration procedures were the same as for the 2.7-m telescope.

Our spectra were not flux-calibrated at the telescope. An adequate calibration was possible using sets of observed *UBVRI* magnitudes (kindly supplied by Yu. S. Efimov and by J. Fernie) in which we interpolated to the dates of our observations. For spectra obtained early in the decline, *UBVRI* magnitudes are unavailable. In these cases, we identified the visual magnitudes as the *V* magnitude. Colours for these early observations were taken from *UBVRI* measurements on earlier declines of R CrB with a similar rate of decline. The range in colours from one decline to another is small and not a major source of uncertainty. Adopted *UBVRI* magnitudes are given in Table 2 for selected dates. Fluxes were

Table 2. Photometry from Efimov (private communication) and Fernie (private communication) of R CrB in the 1995–96 decline.

	Date	*U*	*B*	*V*	*R*	*I*
1995	Oct 18	10.0	10.5	10.1	9.6	9.0
	Nov 2	12.59	12.79	12.02	11.52	…
1996	Jan 5	13.67	14.05	13.57	13.05	12.07
	Feb 6	13.50	14.00	13.50	13.02	11.75
	Mar 2	13.45	13.92	13.45	12.78	11.40
	Apr 9	13.15	13.35	12.47	11.50	10.38
	May 5	12.13	11.67	10.40	9.50	8.68

computed from these magnitudes using Wamsteker's (1981) calibration. Clayton et al. (1997) published a flux-calibrated low-resolution spectrum taken on 1996 April 7. Our derived fluxes for 1996 April 9 are in good agreement with these published values.

3 MAXIMUM LIGHT

R CrB is known to be variable at maximum light. Photometric monitoring of R CrB principally by Fernie and colleagues is providing ample evidence of a continuous quasi-regular variation in light (Fernie 1989, 1991, private communication; Fernie & Seager 1994). Variability of the absorption-line spectrum was detected long ago (Espin 1890). Recent observations at low (Clayton et al. 1995) and high spectral resolution (Rao & Lambert 1997) have begun to detail the changes.

3.1 Photospheric radial velocity

Our measurements of the photospheric radial velocity are based on a selection of 20 to 30 lines that we divide into two groups. Group A comprises high-excitation *weak* lines of N I, O I, Al II and S I. Group B is made up of *strong* lines of C I, O I, Si II, Ca I, K I, Cr II and Ba II. Velocities are derived from the central core of a line. Table 3 and Fig. 1 summarize these measurements covering 558 d from about 8 months before the decline to near complete recovery to maximum light.

At maximum light, the mean velocity of $22.5 \pm 2.0\,\mathrm{km\,s^{-1}}$ and the range of $6\,\mathrm{km\,s^{-1}}$ from observations made between 1995 January and August are the expected values for the star based upon earlier studies (cf. Raveendran, Ashoka & Rao 1986; Fernie & Lawson 1993; Rao & Lambert 1997). Throughout this interval, group A and B lines give the same velocity.

The historical data on the radial velocity of R CrB were searched for a dominant period. We collated radial velocity measurements based on spectra of coudé dispersion – see Keenan & Greenstein (1963), Rao (1974), Fernie, Sherwood & Dupuy (1972), Gorynya, Rastorguev & Samus (1992), Fernie & Lawson (1993) and Rao & Lambert (1997). The set comprises 149 measurements from 1942 to 1995 when the star was not in decline. The dominant source of velocity variations is, of course, the atmospheric pulsation. Our periodogram analysis indicated a pulsation period near 42.7 d. Experimentation with periods around this value suggests that a period of 42.6968 d, a mean velocity of $22.5\,\mathrm{km\,s^{-1}}$ and a range of $6\,\mathrm{km\,s^{-1}}$ provide the best fit to the measurements over the half-century. Several investigators have mentioned that the pulsational period is not strictly constant: a particular value may represent the photometric data for an interval of 1–2 yr. Slight variations of this period or small phase shifts

Table 3. Radial velocities of photospheric absorption lines.

Date	JD−244 0000	All V	All n	Group A V	Group A n	Group B V	Group B n
1995 Jan 24	9742.01	21.2	22	21.0	9	21.3	13
Feb 20	9768.97	24.3	16	24.0	9	24.7	7
Feb 23	9771.92	25.4	17	25.1	9	25.8	8
Mar 17	9793.96	20.1	17	19.8	9	20.5	8
Mar 19	9796.02	21.4	15	20.4	7	22.3	8
Mar 20	9797.00	21.3	14	20.3	7	22.4	7
Apr 14	9821.80	23.8	22	22.5	9	24.7	13
Apr 18	9825.81	26.6	24	25.1	11	28.0	13
Apr 21	9828.78	23.2	22	21.6	10	24.6	12
May 15	9852.85	24.1	24	22.5	10	25.0	14
May 18	9855.82	24.3	25	23.7	10	24.7	10
May 21	9858.80	25.3	3	…	…	25.3	3
May 22	9859.70	25.6	2	…	…	25.6	2
Jun 10	9878.64	19.7	21	19.2	21	20.0	13
Jun 17	9885.64	21.0	27	20.2	10	21.4	17
Jun 19	9887.68	21.2	26	20.6	12	21.4	14
Jun 23	9891.69	21.0	21	19.8	10	21.8	11
Aug 7	9936.61	21.5	26	20.9	12	22.0	14
Aug 8	9937.62	22.8	26	22.0	11	23.0	15
Aug 9	9938.61	23.7	29	23.2	13	…	…
Sep 30	9990.62	…	…	19.9	13	24.8	16
Oct 2	9992.64	…	…	22.6	12	26.4	16
Oct 7	9997.57	…	…	…	…	…	…
Oct 8	9998.55	…	…	…	…	…	…
Oct 9	9999.56	…	…	18.8	7	24.8	10
Oct 11	10001.55	…	…	18.7	9	27.3	11
Oct 12	10002.55	…	…	19.4	9	29.9	7
Oct 13	10003.59	22.9	26	17.9	13	29.5	12
Oct 14	10004.56	14.9	16	14.6	14	17.0	2
Oct 15	10005.55	15.0	16	14.8	14	15.9	2
Oct 18	10008.56	14.4	14	14.0	13	13.5	1
Nov 2	10023.54	15.0	15	16.0	11	14.0	4
Nov 12	10033.54	15.8	5	15.3	2	16.9	3
Nov 14	10035.54	13.6	2	…	…	13.6	2
1996 Jan 5	10088.00	32.8	13	33.6	5	32.3	8
Jan 19	10101.97	37.0	5	35.7	2	37.9	3
Feb 1	10114.96	28.1	5	26.9	4	27.8	1
Feb 6	10119.99	26.5	9	26.5	9	…	…
Feb 8	10122.01	31.4	8	31.8	3	31.2	5
Feb 9	10123.01	30.4	8	29.7	4	30.4	4
Mar 2	10144.95	30.6	10	30.8	7	29.9	3
Mar 10	10152.99	34.0	3	…	…	34.0	3
Mar 13	10155.90	34.5	2	…	…	34.5	2
Apr 9	10182.74	28.5	10	28.6	5	27.9	5
Apr 9	10182.77	28.3	13	27.2	5	29.3	8
May 3	10206.90	28.7	13	28.5	8	29.0	5
May 4	10207.88	29.1	19	28.4	10	29.9	10
May 5	10208.85	29.5	19	29.2	9	29.8	10
May 6	10209.85	29.3	19	29.0	9	29.5	10
May 9	10212.82	25.5	13	24.5	7	26.7	6
May 9	10212.83	25.5	19	24.4	7	26.2	12
May 31	10234.78	20.5	19	21.1	7	20.2	12
Jun 4	10238.77	21.5	19	21.6	7	21.4	12
Jun 5	10239.63	21.9	24	21.9	10	21.9	14
Jun 25	10259.72	23.1	13	21.9	7	24.8	6
Jul 8	10272.73	20.3	22	21.6	7	19.7	15
Jul 23	10287.65	17.1	25	15.8	10	18.1	15
Jul 24	10288.61	16.4	22	15.0	11	17.8	11
Jul 26	10290.64	16.0	14	15.4	8	17.3	6

[a] Velocity V is given in km s^{-1}, followed by the number of lines n.

the A lines where there is a significant difference; the open squares denote group B velocities where they differ from the A velocities by more than $2\,\mathrm{km\,s^{-1}}$. The line is the 'historical' sine curve with a period of 42.6968 d and a range of $6\,\mathrm{km\,s^{-1}}$ around a mean velocity of $22.5\,\mathrm{km\,s^{-1}}$. (The difference between periods of 42.6968 and 42.7588 d is unimportant over this short interval of time). Observations prior to the onset of the decline are closely matched by the sine curve.

Both group A and B lines depart in different ways from this curve at the onset, but the difference between group A and B lines disappears after a few days. Then, the radial velocity shown by photospheric (group A and B) lines is systematically more positive throughout the deepest part of the decline than predicted by the sine curve. These deviations occur at a time when the absorption lines have very unusual profiles. Lines unaffected by emission show shallow asymmetric profiles quite unlike photospheric profiles seen at maximum light. These changes and the marked redshift are attributed to scattering of photospheric light by the dusty envelope of R CrB (Section 9.3). We presume that the obscured photosphere pulsated throughout according to the sine curve shown in Fig. 1. The two measurements from late in the recovery match well the predicted sine curve, showing that the pulsation after the decline followed the ephemeris that matched the pre-decline observations. These observations indicate that, except for the photospheric disturbance at the onset (Section 4), the photosphere pulsated, oblivious to the cloud of soot obscuring it from our view.

3.2 Sharp emission lines at maximum light

At maximum light, strong low-excitation lines of neutral atoms and singly charged ions show an apparent doubling in their absorption cores, as first seen by Payne-Gaposchkin (1963) and Keenan & Greenstein (1963), and confirmed from high-resolution CCD spectra by Lambert et al. (1990). The doubling is considered to result from the superposition of an emission component on the photospheric absorption core. Our present spectra confirm that the emission is probably a permanent feature at maximum light. An excellent spectrum obtained on 1995 May 18 clearly shows emission in Sc II 4246 Å, Sr II 4077 and 4215 Å, the Na I D lines, and the Ca II infrared triplet lines, representing the emission spectrum E2. The emission is at a velocity of $18 \pm 1\,\mathrm{km\,s^{-1}}$ or shifted to the blue by about $5\,\mathrm{km\,s^{-1}}$ relative to the systemic velocity of the photosphere. Fig. 2 shows the Sc II 4246-Å line on three occasions in 1995 prior to the decline, two occasions right at the onset of the decline, and when the star had faded by about 1.6 mag. The emission core is present prior to onset with an intensity that appears slightly variable, but this variation may reflect a varying continuum flux resulting from the pulsation. Emission at the same velocity is striking in the 1995 October 13 spectrum. Continuing the sequence, Fig. 3 shows the May 18 maximum light spectrum, the October 13 spectrum, and the October 18 spectrum when the star had faded by 4 mag. On this latter spectrum, weaker emission is clearly present in all the photospheric lines in this region. Incipient emission is present affecting these lines in the October 13 spectrum shown in Fig. 2.

Our inference is that sharp emission lines are a permanent presence. As we show below, these sharp emission lines are of constant velocity, unreddened, and of constant flux until the photosphere is dimmed by about 4 mag. These are surely clues to the location of the emitting region of the lines.

seem to be indicated. For example, if the earliest measurements assembled by Keenan & Greenstein (1963) are dropped, the best-fitting period is lengthened slightly to 42.7588 d.

In Fig. 1, we show the measured velocities: filled circles denote either the mean velocity of group A and B lines where there is no significant difference between the two groups, or the velocity of
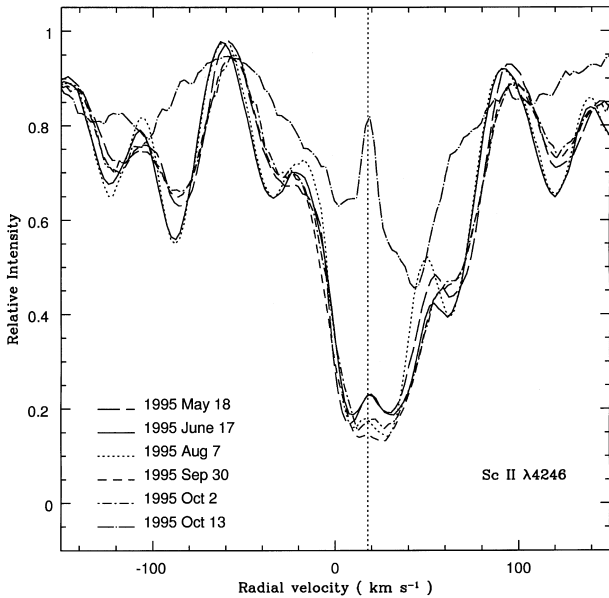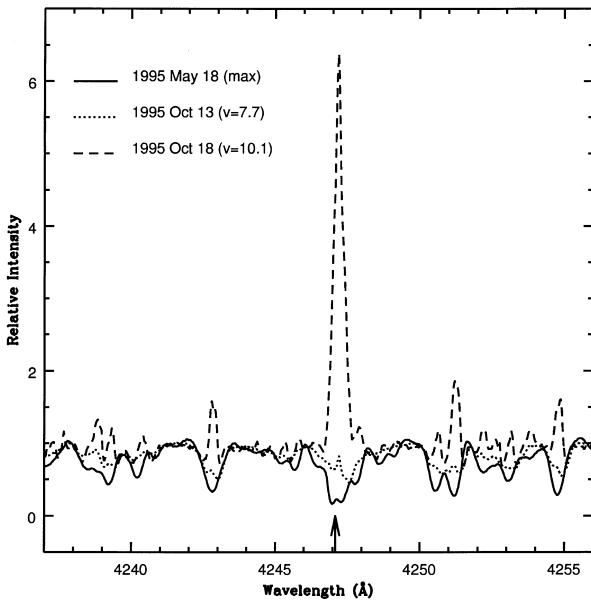
Figure 2. The central emission core of the Sc II 4246-Å line on five occasions prior to the 1995 decline, and on 1993 October 13 when the star had faded by 1.6 mag. The vertical broken line denotes a radical velocity of $18 \, \text{km s}^{-1}$.

Figure 3. The emergence of the sharp emission-line spectrum near Sc II 4246 Å. The key indicates when these spectra were obtained and the visual magnitude on those dates.

4   THE ONSET OF THE DECLINE: PHOTOSPHERIC ACTIVITY

Our spectra reveal remarkable changes in high-excitation photospheric lines over an interval of a fortnight beginning with the onset of the decline. It seems probable that the changes betray information about the mysterious trigger of an RCB decline. In particular, this discovery sites the trigger in the stellar photosphere and eliminates some ideas about the cause of the decline: i.e. the decline is not brought on by passage of a circumstellar cloud
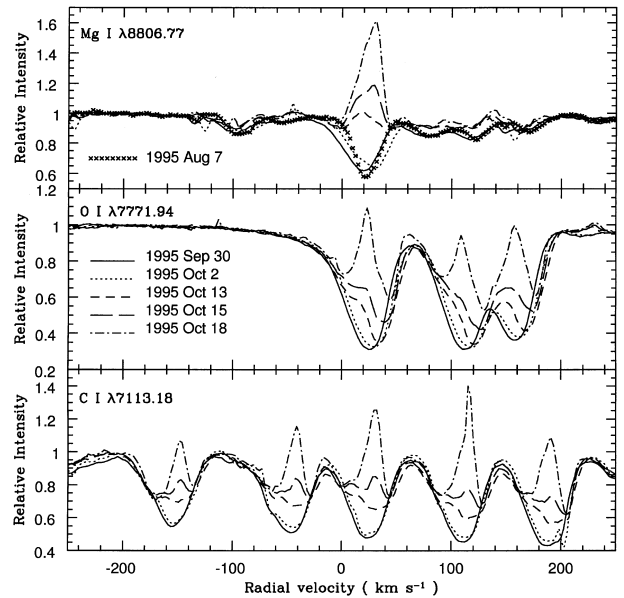
Figure 4. Profiles of high-excitation lines from onset of the decline near 1995 September 30 through to 1995 October 18 when R CrB had faded to $V \simeq 10$. The top panel shows the Mg I 8806-Å line. The middle panel shows the O I triplet with the velocity scale set to the 7771.94-Å line. The bottom panel shows C I lines near 7100 Å with the velocity scale set to the 7113.18-Å line.

across the disc of the star, or by spontaneous condensation of soot in the cool outer reaches of the atmosphere.

The changes are well illustrated in Fig. 4, showing comparisons of the spectra obtained on 1995 September 30 and August 7. On September 30 R CrB remained close to maximum light, but by October 2, the date on which the next spectrum was acquired, it had begun to fade. Beginning with the September 30 spectrum, there is a clear velocity difference (Table 3, Fig. 1) between the group A and B photospheric lines, as measured from their line cores. Unfortunately, it is not possible to date precisely the onset of this velocity difference, except to note that it was not present from August 7 to 9. The difference increased almost monotonically from about $5 \, \text{km s}^{-1}$ on 1995 September 30 to about $12 \, \text{km s}^{-1}$ by 1995 October 13 when the star had faded to $V \simeq 7.7$. Since the group B lines are formed closer to the surface than the group A lines, we infer that shallower photospheric layers were falling in towards the deepest visible layers at velocities in excess of the sound speed ($\simeq 5 \, \text{km s}^{-1}$). Shortly after October 13, emission appeared in the core of a group B line (Fig. 4). Transition from a broader than usual absorption line to an emission line in the wing of an absorption line occurred between 1995 October 9 and 13. Emission persisted to just prior to 1995 November 2 ($V \simeq 12$), when the profiles of group B lines again resembled photospheric lines observed near maximum light, and the velocity difference between group A and B lines was less than $2 \, \text{km s}^{-1}$ with a mean velocity blueshifted by about $8 \, \text{km s}^{-1}$ relative to the systemic velocity. These emission lines belong to the class of E1 lines.

In late September, the photospheric velocities according to the 42.6968-d sine curve should have been close to their maximum value of about $26 \, \text{km s}^{-1}$. Lines of group B, the strong to very strong lines of C I, O I and other species, are close to the expected velocity, but lines of group A, high-excitation weak lines of N I and other species, are blueshifted with respect to the predicted maximum velocity. Group B lines on September 30 are also

broadened relative to their August 7 profiles, and to the group A profiles in this early phase of the decline. For all lines, the red wing remains at about the same velocity but there is additional absorption on the blue side of group B lines. In contrast, the group A profiles are largely unchanged, although shifted in velocity. Although the group B lines later show an emission component, it is unlikely that these differences in profile are initially or solely due to emission altering an underlying unchanging absorption profile, because the equivalent widths of the affected lines are larger on September 30 than on August 9. The profile changes during onset of the decline are considerably more extreme than those occurring during regular pulsations at maximum light (Rao & Lambert 1997).

These emission lines associated with the onset – the 'transient' or E1 lines – are to be distinguished from the sharp emission (E2) lines present in and out of a decline. A distinguishing feature of the onset-related or transient emission lines is their large range of excitation potential. At the top end are lines with lower excitation potential in the range 6.5 to 9.5 eV. Such lines are *not* contributors of sharp (E2) lines. Lines of lower excitation potential are blends of a transient and a sharp line, and include Li I, Ca I, Fe II, Ni I and La II transitions. Another notable contributor of transient but not sharp lines is the C_2 Swan system (see below). Significantly, group A lines do not appear in emission. The fluxes of the C I transient emission lines provide an estimate of the excitation temperature. The strongest lines are optically thick in that lines from the same multiplet do not scale with the *gf*-values of the lines. Lines that do appear to be optically thin suggest an excitation temperature of about 8400 K. This temperature is definitely higher than that estimated from the sharp emission lines. The velocity of the transient C I emission lines is 20 to 30 km s^{-1}, i.e. a velocity between that of the group A absorption lines and the redshifted absorption component accompanying transient emission lines.

On 1995 October 18 almost all lines showed a red absorption component or an inverse P Cygni profile.[1] Fig. 5 is a montage of emission lines with the redshifted absorption indicated. Many lines are a blend of transient and sharp emission components at a very similar velocity. The red absorption component is not a portion of the photospheric line not filled in by emission. This assertion is based on the fact that the full array of lines gives the same velocity for this component: 43 km s^{-1} from 90 lines, or a redshift of 30 km s^{-1} with respect to the mean velocity of group A and B lines or 20 km s^{-1} relative to the systemic velocity of the photosphere. If the red absorption were a residual of the photospheric line, we would expect the apparent velocity to vary with the strength of the overlying emission. More significantly, the depth of the red absorption for many lines is deeper than the photospheric line depth at the same velocity from the line core, as clearly seen in the Ba II 5854-Å line (Fig. 6). The redshifted absorption is also a transient phenomenon, and by 1995 November 2 had disappeared.

Curiously, a few lines, e.g. Ni I 7789 Å (Fig. 7), exhibit a P Cygni profile with the absorption component at the photospheric velocity. Oddly, P Cygni profiles appear restricted to a few Ni I multiplets and high multiplets of Fe I (e.g. RMT1107). The P Cygni profile was not seen on or after 1995 November 2. The difference between P Cygni and inverse P Cygni profiles could be

[1] Inverse P Cygni profiles for low-excitation lines were observed by Vanture & Wallerstein (1995) on a spectrum of RY Sgr taken during the recovery from its 1993 deep minimum. High-excitation lines were not seen in this spectrum.
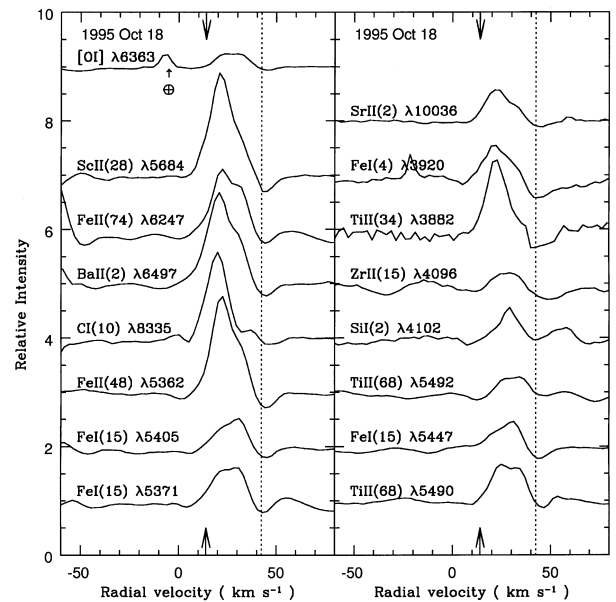
Figure 5. Selected emission lines from the 1995 October 18 spectrum. The photospheric velocity, as measured from lines without an obvious emission component, is indicated by the arrow top and bottom of the figure. Most lines have a redshifted absorption component at 43 km s^{-1} which is indicated by the dotted line.
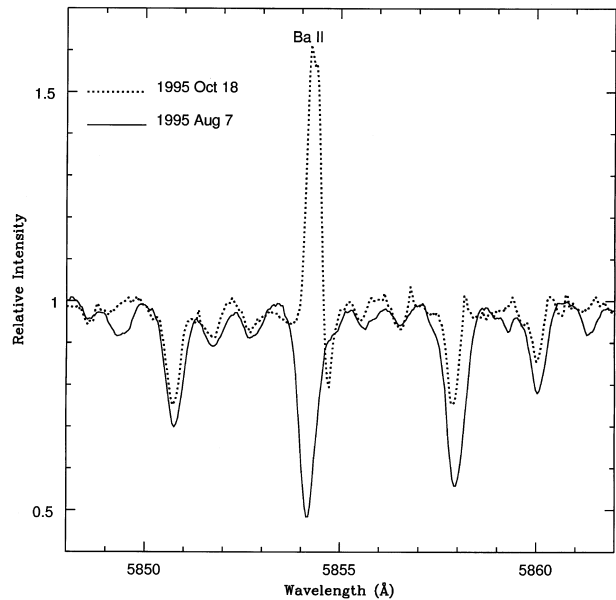

Figure 6. The Ba II 5854-Å line on 1995 August 7 prior to the decline and on 1995 October 18 when the star had faded by 4 mag. Spectra have been aligned so that the weaker photospheric lines are superimposed. Note the depth of the sharp absorption associated in the Ba II line red wing.

due to a velocity differential between the layer providing the absorption line and that providing the emission line. Since the latter appears at about the same velocity for all lines, the absorption line is shifting such that weak lines (e.g. Ni I) formed at the top of the photosphere are blueshifted relative to lines formed deeper in the atmosphere (e.g. O I); the velocity shifting to more positive velocities for lines formed at shallower depths in the photosphere.
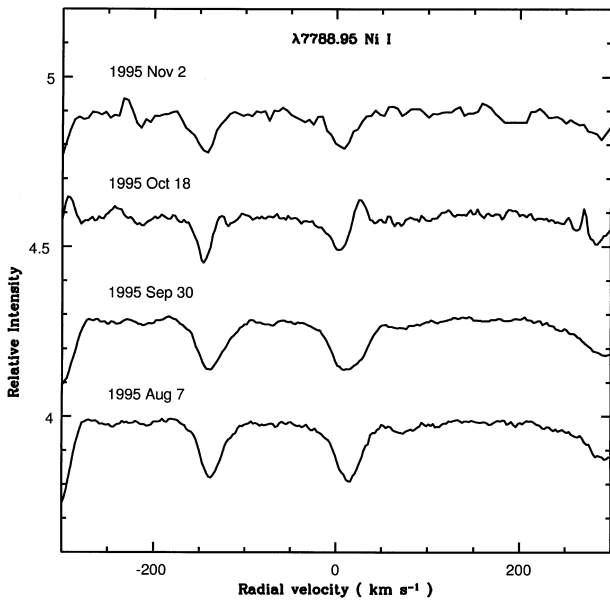
Figure 7. Evolution of the Ni I line at 7789 Å from prior to the decline through to 1995 November 2 when the star had faded by about 6 mag. Note the P Cygni profile on 1995 October 18 and the disappearance of emission by 1995 November 2.
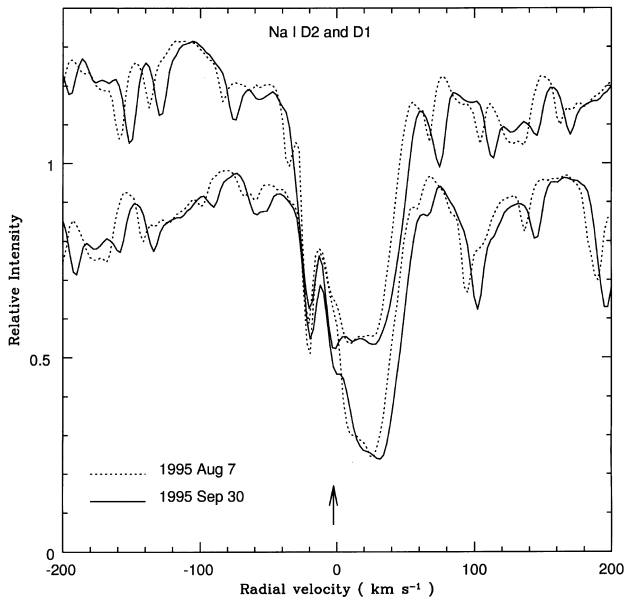
Figure 8. Profiles of the Na I D_1 and D_2 lines on 1995 August 7 and September 30. The August 7 spectrum was obtained at maximum light. Additional absorption (marked by the arrow) appears in the September 30 spectrum when the decline was just beginning. The sharper component to the blue is a permanent unchanging interstellar (or circumstellar) pair of unresolved lines. Spectra have been aligned such that this interstellar component is at its heliocentric velocity. Weak sharp lines that seem to be different in the two spectra are telluric H_2O lines.

An additional absorption component is seen in the strong Na I D lines following the onset of the decline. In addition to changes in their photospheric profiles, the Na I D lines showed on 1995 September 30 additional absorption in their blue wing (Fig. 8). (Similar changes occurred in the Ca II infrared triplet lines.) This absorption, which appears to be a narrow component, is at about

$-3 \, \mathrm{km \, s^{-1}}$ or blueshifted by nearly $30 \, \mathrm{km \, s^{-1}}$ relative to the anticipated photospheric velocity.

Our spectra show that membership in the E1 class of emission lines must be extended to include high-excitation lines of C I, O I and other species.[2] The primary factor behind the evolution of the E1 spectrum is the changing physical conditions in the emitting regions, and not the occultation of these regions by the developing dust cloud. The mix of line profiles from P Cygni to inverse P Cygni is difficult to understand if occultation by remote dust is dominant, but more readily understood if the transient lines are emitted by atmospheric layers experiencing shocks. Emission in the high-excitation lines lasts a brief while. At its disappearance, the absorption profiles are returned to their pre-decline condition (see below) because, we suggest, the disturbed atmospheric layers have relaxed to approximately their normal state. If occultation by the fresh dust cloud were to control the appearance of the transient lines, it would be necessary to suppose that the optical depth to the photosphere were less than that to the emitting region of the lines. This seems unlikely. Moreover, shock-excited C I emissions are present in RY Sgr during its pulsation cycle (Cottrell & Lambert, unpublished observations) at maximum light, similar to the emission seen above. If future observations show that the behaviour of high-excitation lines in 1995 was typical of all declines, an explanation in terms of occultation by dust will be excludable.

5 R CrB AROUND MINIMUM LIGHT: THE SHARP EMISSION-LINE SPECTRUM

5.1 Introduction

After 1995 November 2 ($V = 12.2$), the emission-line spectrum comprises low-excitation lines of mainly singly ionized metals. Representative line profiles are shown in Fig. 5 for 1995 October 18: the C I 8335-Å line is a transient line, but lines such as Fe I 5405 and 5371 Å are sharp lines. Evolution of the emission-line spectrum is shown by Figs 9 and 10.

The sharp emission lines appear composed of two or three components which we label C1, C2 and C3 in order of increasing velocity. The lines are resolved; the instrumental (FWHM) width as measured from the Th comparison lines is about $5 \, \mathrm{km \, s^{-1}}$ but the C2 component has a FWHM of about $14 \, \mathrm{km \, s^{-1}}$. The emission lines are not broader than the same lines in absorption at maximum light: the base widths of the emission and absorption lines are both about $40 \, \mathrm{km \, s^{-1}}$. The principal component (C2) is at $20 \, \mathrm{km \, s^{-1}}$ or displaced by $-3 \, \mathrm{km \, s^{-1}}$ from the systemic velocity. This shift is slightly smaller than reported at earlier declines for R CrB and RY Sgr.
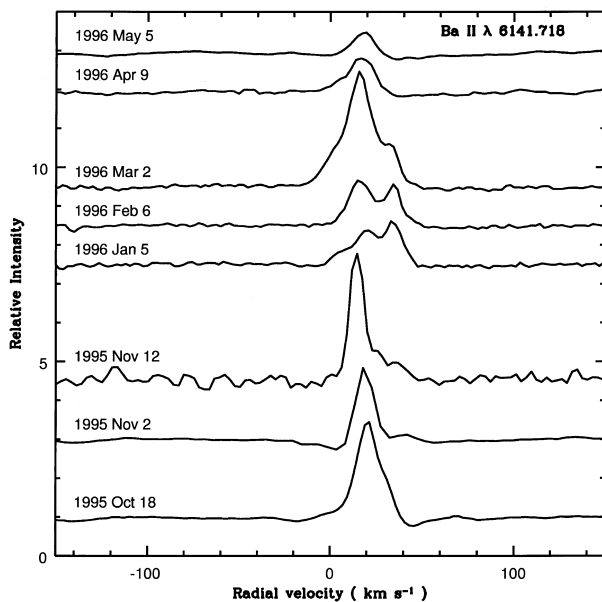
5.2 Forbidden lines

In all previous discussions of the sharp-emission-line spectrum of R CrB stars in decline, identified lines were exclusively permitted lines. Indeed, permitted lines comprise the vast majority of sharp lines in our spectra. Searches for forbidden lines, where reported, were described as unsuccessful. Since forbidden lines may provide data on physical conditions in the emitting gas, we searched for a variety of forbidden lines.

---

[2] Some earlier reports based on photographic spectra did note a filling-in of C I lines in the blue, but red lines were not observed photographically. Our spectra show transient weak emission cores in the stronger C I lines in the blue (e.g. RMT6 at 4762–4776 Å).
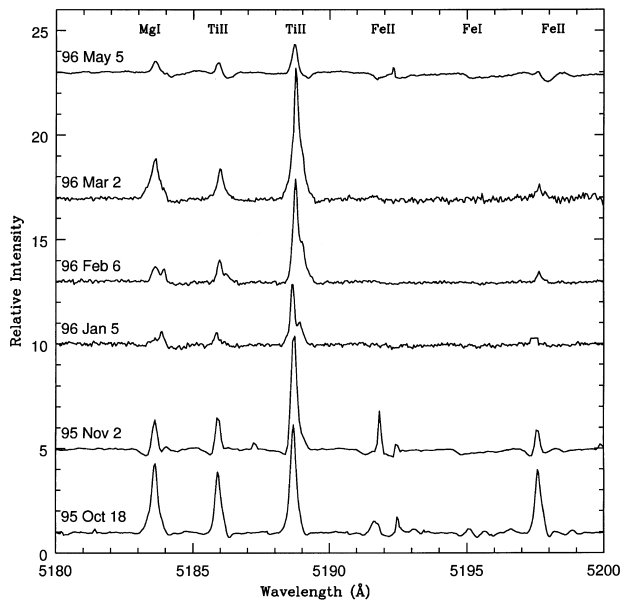
Figure 9. Sharp emission lines on representative spectra from early in the decline to late in the recovery.

Figure 10. Evolution of the Ba II 6142-Å line from early in the decline to late in the recovery.

We have identified sharp forbidden lines for the first time. Identifications include [C I] 8727, 9823 and 9850 Å, [O I] 5577, 6300 and 6363 Å, and [Ca II] 7291 and 7323 Å,[3] and several detections of [Fe II] lines. Forbidden lines have the profile (component structure) and the velocity of the permitted sharp lines.

[3] [Ca II] lines had been identified previously in the 1977 decline of R CrB (Herbig, private communication) and in RY Sgr by Asplund (1995), but the spectral resolution did not permit a clear differentiation between sharp and broad emission in these lines. The [O II] 3727-Å line must have been present but our spectra have too low a signal-to-noise ratio at that wavelength.
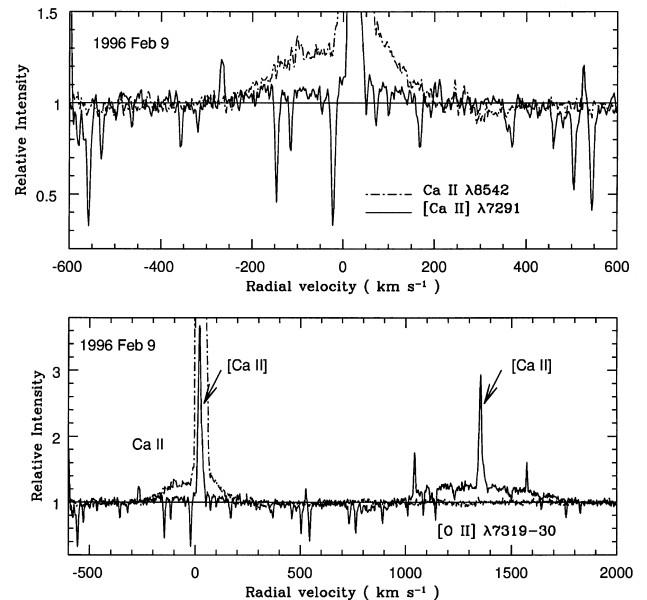
Figure 11. The [Ca II] lines at 7291 and 7323 Å. The top panel shows the 7291-Å line and the infrared triplet 8542-Å line. The latter line has a strong sharp component not fully shown and a broad component. The [Ca II] 7291-Å line has a sharp component also not fully shown and a hint of a broad component. Sharp lines across the 7291-Å spectrum are telluric H$_2$O lines. The lower panel for which the velocity scale is set to the 7291-Å line rest wavelength of 7291.46 Å shows both forbidden lines. The broad emission around the [Ca II] 7323-Å line is a blend of [O II] lines.

[C I]. The 9850-Å [C I] line was seen first on 1995 October 13 and was last seen on 1996 May 5. The excited 8727-Å line was present on 1995 October 13 but unfortunately later spectra did not include this wavelength region. The estimated flux ratio for 1995 October 13 is $F(8727)/[F(9850) + F(9823)] = 2.4 \pm 0.3$, where the contribution of the 9823-Å line is estimated from that of 9850 Å and the known branching ratio.

[O I]. The lines 6300, 6363 and 5577 Å are present. The 6363-Å line (Fig. 5) was first seen on 1995 October 15, and like the [C I] 9850-Å line was present throughout the decline. We estimate that the flux ratio $[F(6300) + F(6363)]/F[5577] \sim 18$ throughout the decline.

[Ca II]. The 7291- and 7323-Å lines are the strongest forbidden lines that are sharp (Fig. 11). Strong sharp components seen for the two forbidden lines and the permitted infrared triplet are superimposed on weak broad emission lines. Relative fluxes in the forbidden and the permitted infrared and H/K lines are discussed below.

[Fe II]. Unsuccessful searches for [Fe II] lines were reported from photographic spectra by Herbig (1949) and Payne-Gaposch-kin (1963) for R CrB in decline, and by Alexander et al. (1972) for RY Sgr. Our spectra show weak [Fe II] emission lines from 1995 October 18 to 1996 February 6. Fig. 12 shows three lines from the 1996 February 6 spectrum. Radial velocities of the lines coincide with that of the central component of the permitted lines. The flux ratio of forbidden and permitted lines evolved with the former becoming relatively stronger until about the middle of the deepest part of the decline. For example, the flux ratio of the 4244-Å [Fe II] and the 4233-Å Fe II lines increased from 0.008 on 1995 October 18 to 0.13 on 1995 November 13 and to 0.45 on 1996 February 6.
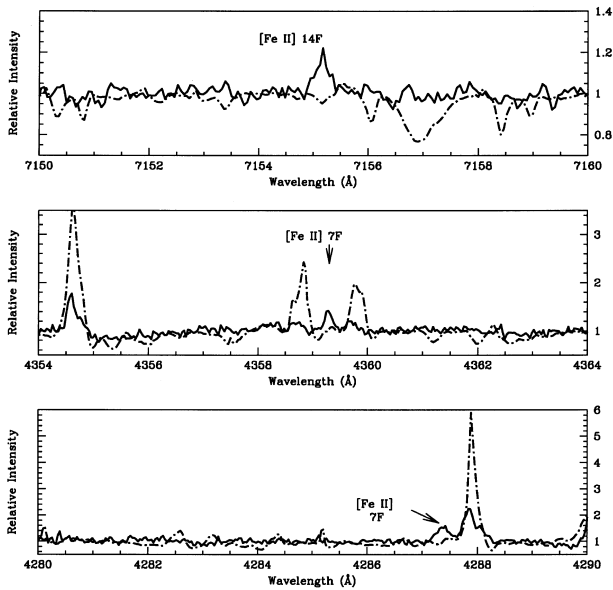
Figure 12. [Fe II] lines in the spectrum of R CrB at minimum light. [Fe II] lines present in the 1996 February 6 spectrum (solid line) are identified. The comparison spectrum for 1995 October 18 (dash–dotted line) does not show these forbidden lines.

5.3 Evolution of sharp emission lines

Our extensive coverage – temporal and spectroscopic – encouraged us to examine fully the rich sharp-line spectrum. Prior to 1995 October 18 and after 1996 May 5, the emission was too weak for reliable measurement and, where present, superimposed on a photospheric line. Observed line profiles were decomposed into their two or three components, assumed here to be Gaussian in form, and equivalent width, FWHM and velocity were measured using IRAF routines for each component. As far as possible, the same lines were measured on each spectrum from 1995 October 18 to 1996 May 5. Decomposition of a complex profile implies perhaps that each component is physically distinct. This is not necessarily so, as the emitting region may be a single geometrical structure with three dominant regions in relative motion. Since the C2 and C3 and possibly the C1 components are present throughout at fixed relative velocities, the structures that they represent would appear to be physically related in some sense, e.g. cloudlets on a uniformly expanding or rotating ring.

The data set is applied to answering the following questions relating to the appearance of the sharp emission lines.

(i) By how much are the components reddened? Obviously, some reddening is interstellar and some circumstellar in origin. Detections of a difference in the reddening of different components or a change during the decline would be exciting clues to the relative location of gas and dust.

(ii) What are the velocities of the components? Is there a change in velocity during the decline? Do the radial velocities and linewidths vary systematically with the type of line, i.e. neutral atom or singly charged ion, low or high upper state excitation potential? Demonstrable variations, or the lack of them, are clues to the relative locations of the emitting gas and the freshly made dust.

(iii) How do the fluxes of the components change during the decline? Is there a reduction in flux that is correlated with the

fading of R CrB during the decline? Again, these measurements offer clues to the locations of emitting gas and absorbing dust.

(iv) What are the physical conditions of the emitting regions? Estimates of temperature and electron density are provided fairly directly from relative fluxes of small or large sets of the emission lines.

The answers to these questions provide clues to the location of the emitting gas in and around R CrB, as we discuss in Section 9.5.

5.3.1 Reddening

In decline, the reduction in flux from the photosphere of an R CrB star is largest in the blue and least in the red (cf. Clayton 1996). This observation implies not unexpectedly that photospheric radiation is dimmed and reddened by small dust particles. Significantly, the emission lines appear to be unaffected by this reddening (cf. Clayton 1996). In the case of R CrB, Payne-Gaposchkin (1963) commented that 'the chromosphere has continued to decline in brightness but is affected slightly (if at all) by the reddening that alters the energy distribution'. An interpretation of this result is that an optically thick dust cloud partially obscures the emitting region; the observed emission comes from the unobscured (i.e. unreddened) parts of the emitting region. Of course, the sharp emission lines are subject to interstellar and circumstellar reddening, but this has been shown to be small for R CrB: $E(B - V) \simeq 0.05$ mag (Rao 1974; Asplund et al. 1997).

Here, we examine whether the different emission-line components are affected by reddening. We exploit the fact that our spectra provide several cases of lines at rather different wavelengths arising from the same upper level. Then there is a simple relation between the emission-line *fluxes* of pairs of optically thin lines:

$$\frac{W_\lambda(1)F_c(\lambda_1)}{W_\lambda(2)F_c(\lambda_2)} = \frac{A(1)\lambda_2}{A(2)\lambda_1}, \tag{1}$$

where W_λ is the equivalent width of a line, $F_c(\lambda)$ is the observed flux in the spectrum at the wavelength of the line having wavelength λ, and A is the transition probability for spontaneous emission in the line.

A set of Ti II lines was chosen. Accurate transition probabilities were taken from Martin, Fuhr & Wiese (1988). Flux ratios of red and blue lines from the same upper state were estimated, and are compared in Table 4 with the predicted ratios for unreddened optically thin lines. When the Ti II lines were resolvable into two or three components, the observed ratio was estimated separately for each component. Inspection of Table 4 shows that the observed ratios are fairly consistent with these predictions which assume *no* reddening. The conclusion is clear. Emission lines are very little reddened by the soot causing the decline: the limit $E(B - V) \leq 0.15$ mag may be set. Note that the photometric colours changed very little until late in the decline: Table 2 shows that $(B - V) \simeq 0.5$ from 1995 October 18 to 1996 March 2, increasing to 0.9 and 1.3 on 1996 April 9 and May 5 respectively.
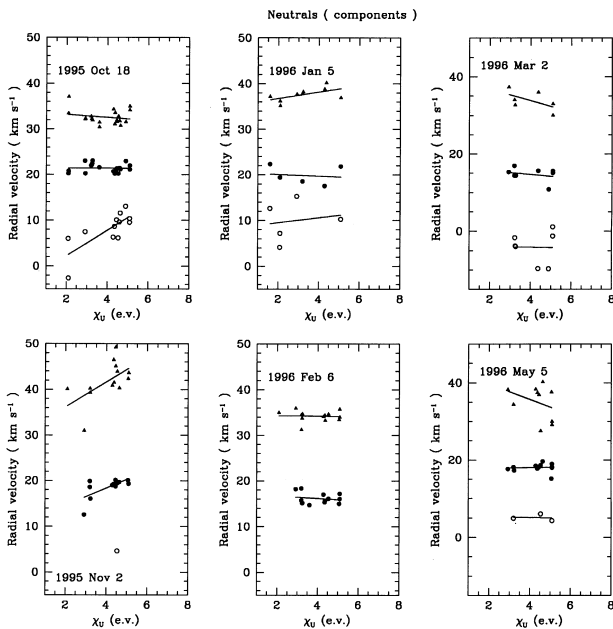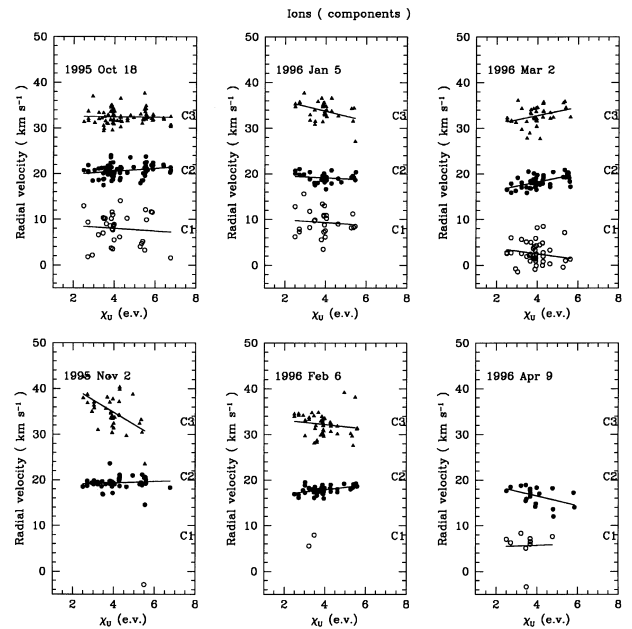
5.3.2 Radial velocities

Radial velocities were measured for a large number of sharp emission lines. When possible, velocities of components C1, C2

Table 4. Observed and predicted flux ratios of Ti II emission lines.

Ratio (λ_1/λ_2)	Predicted ratio	Observed ratio Date													
		95 Oct 18			95 Nov 2		96 Jan 5			96 Feb 6		96 Mar 2			96 May 5
		C1	C2	C3	C2	C3	C1	C2	C3	C2	C3	C1	C2	C3	C2
6492/4341	0.42	…	0.48	…	0.21	…	…	0.35	…	0.42	…	…	…	…	0.37
8979/4341	0.10	…	0.09	…	…	…	…	…	…	…	…	…	…	…	…
5189/4533	0.28	…	…	…	0.42	0.28	0.24	0.43	0.31	…	…	0.54	0.33	0.32	…
6491/4534	0.022	…	…	…	0.03	…	…	0.05	…	…	…	0.10	0.04	…	0.10
6491/5189	0.08	…	…	…	0.07	…	…	0.11	…	0.12	0.07	0.19	0.13	0.06	0.22
5129/5186	1.05	0.99	0.82	1.28	…	…	…	…	…	0.91	1.20	1.00	1.05	1.10	…

Table 5. Radial velocities (km s^{-1}) of emission lines.

Date		JD -2440000	Sharp lines			Broad lines		
			C1	C2	C3	He I 7065 Å	He I 3889 Å	[N II] 6583 Å
1995	Oct 18	10008.56	6.0	20.1	32.0	-8.8	…	…
	Nov 2	10023.54	…	19.3	35.0	-7.9	…	…
	Nov 12	10033.54	…	…	…	-8.7	…	-14.4
1996	Jan 5	10088.00	9.0	19.0	33.5	-2.6	-5.6	1.1
	Feb 6	10119.99	…	17.7	32.0	-4.9	-14.4	-3.6
	Feb 9	10123.01	…	…	…	…	…	-14.8
	Mar 2	10144.95	3.8	18.2	32.8	-7.9	-10.3	…
	Apr 9	10182.74	8.5	18.0	…	…	…	…
	May 5	10208.85	6.7	18.3	42.2	…	1.1	…

Figure 13. Variation of radial velocity with upper excitation potential (χ_u) for the three components of the emission lines of neutral atoms. Velocities of the components C1 (blue), C2 (central) and C3 (red) are shown for selected dates. Straight lines are the least-squares fits to the data.

Figure 14. Variation of radial velocity with upper excitation potential (χ_u) for the three components of the emission lines of singly charged ions. Velocities of the components C1 (blue), C2 (central) and C3 (red) are shown for selected dates. Straight lines are the least-squares fits to the data.

and C3 were recorded along with the FWHM. Measurements were grouped by species (neutrals and ions) and excitation potential of the emitting level (χ_u). Results are summarized in Table 5. Measurements for selected dates are shown as a function of χ_u in Fig. 13 for neutral atoms and Fig. 14 for singly charged ions.

The mean velocity of the central and often dominant C2 component is 18 ± 2 km s^{-1}, corresponding to a blueshift of about 4 km s^{-1} relative to the systemic velocity. When the components

are well sampled, the velocity separation of C3 (red) from C2 (central) is 15 ± 2 km s^{-1}, and that of C1 (blue) from C2 (central) is 11 ± 2 km s^{-1}. Thus the separations of the outer components from the central one are approximately equal. Perhaps more importantly the average velocity of the C1 and C3 components is the systemic velocity to within the errors of measurement. The absolute velocities evolve only slightly, if at all, from the first appearance of the emission lines to late in the recovery. The

Ions (FWHM components)
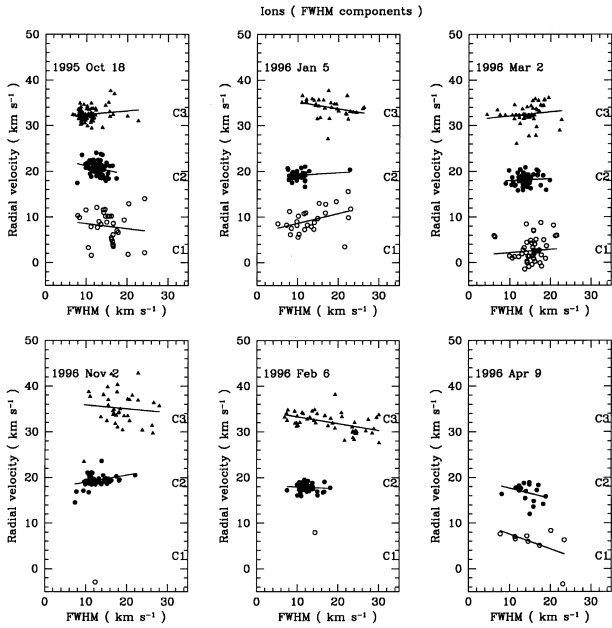
Figure 15. Radial velocity versus linewidth (FWHM) for emission lines of singly charged ions for the three components C1, C2 and C3. The straight lines are least-squares fits to the data.

observed range in velocity of the C2 component is at most about $3\,\mathrm{km\,s^{-1}}$ (Table 5), declining from $20\,\mathrm{km\,s^{-1}}$ on 1995 October 18 to $18\,\mathrm{km\,s^{-1}}$ during and after the deepest part of the decline. The radial velocity of a component on a given date is the same for neutrals and ions and is independent of χ_u and line flux. A weak velocity gradient with χ_u may be present on occasion.

Neutral and ionized lines have similar FWHM on the same spectrum. Measurements of the FWHM of the ionized lines are summarized in Fig. 15. The few neutral lines suitable for measurement hint at a larger linewidth on occasion, but this may reflect a bias in measuring broader and probably stronger neutral lines; the difference is not more than about $3\,\mathrm{km\,s^{-1}}$. The FWHM of C2 lines is the same for all lines, independent of species and χ_u. The distribution of measurements off a single spectrum is consistent with a very narrow distribution of the intrinsic FWHM. The mean FWHM of C2 varies very little from one observation to another and has a mean value of $10–14\,\mathrm{km\,s^{-1}}$ uncorrected for the instrumental broadening of nominally $5\,\mathrm{km\,s^{-1}}$. FWHM measurements for C1 and C3 show a broader distribution which reflects in part the difficulty of measuring these often weaker components. On average, their mean FWHM is similar to that of the C2 component, but there are some real differences: the FWHM of C3 is less than that of C2 on 1995 October 18, and the distribution of FWHM for C3 and possibly C1 is distinctly broader than for C2 during the deepest part of the decline (see Fig. 15 for 1996 January 5 and February 6).

5.3.3 Time-dependent flux variations

As Fig. 9 clearly shows, the integrated flux of a sharp line does not decline in step with the diminution of the photospheric flux; the equivalent width of a line would remain constant in the event that line and photosphere were similarly affected. The difference between the two is striking. Measurements of selected lines show that the integrated flux of a line is approximately the same on 1995 October 18 as in the pre-decline maximum light spectrum of

1995 May 18, despite the fading from $V = 5.9$ to 10.1, a factor of 50. By 1995 November 2 and $V = 12.2$, the line flux had declined by 50 per cent as the star had faded by a factor of 330 from maximum light. At its faintest, the star was at $V \simeq 13.5$ or a factor of 1100 below maximum light, yet the line flux had been reduced not to 0.09 per cent of its 1995 October 18 value but only to 8 per cent on 1996 January 6, 13 per cent on 1996 February 6 and 22 per cent on 1996 March 2. This increasing trend continued, reaching 30 per cent on 1996 May 5. This extraordinary difference between 'continuum' and lines is a valuable clue to the relative locations of the obscuring soot cloud and the emitting region of the sharp lines. (Our use of photometric magnitudes to calibrate the continuum fluxes assumes that the lines in a photometric bandpass do not contribute an appreciable amount of flux. This is certainly the case for the V and R bandpasses.)

Inspection shows that flux ratio of the components C2 and C3 is not constant throughout the decline. At minimum light, the ratio C3/C2 is about 0.8 according to measurements of the spectra of 1996 January 5 and February 6. Spectra from early in the decline (1995 October 18 and November 2) and in the recovery phase (1996 April 9 and May 5) show a stronger C2 component with a C3/C2 of about 0.3. The spectrum of 1996 March 2 gives an intermediate ratio of about 0.4. There is a hint in the measurements that the ratio C3/C2 is larger for lines of low χ_u. These results are well shown by the evolution of the Ba II 6142-Å line (Fig. 10). The C1 component, which is less clearly seen, may retain a constant flux ratio C1/C2 over the entire decline.

5.4 Physical conditions in the emitting region

Ratios of line fluxes provide estimates of the physical conditions (temperature and density) of the emitting gas. Since the line profiles are independent of species and the excitation potential, and similar across the collection of spectra, it is reasonable to suppose that the gas is reasonably homogeneous and that estimates obtained from one species are widely applicable.

Forbidden lines are well-known diagnostics. For the interpretation of the [C I] and [O I] line ratios we use a program written by Surendiranath (private communication) based on collision strengths from Mendoza (1983). Temperature $T \simeq 4000\,\mathrm{K}$ and electron density $n_e \simeq 1 \times 10^7\,\mathrm{cm^{-3}}$ are indicated by the [C I] ratio given in Section 5.2. The corresponding [O I] ratio implies that $T \simeq 5000\,\mathrm{K}$ and $n_e \simeq 5 \times 10^7\,\mathrm{cm^{-3}}$. These results are in fair agreement considering that our spectra were not directly flux-calibrated. The emitting region is warm and fairly dense.

Fluxes of the permitted lines were analysed to obtain excitation temperatures. We considered the species Ti II, Fe I and Fe II which are well represented by sharp emission lines and for which reliable transition probabilities are available. These were taken from Martin et al. (1988) for Ti II, and from Lambert et al. (1996) for Fe I and Fe II. We found that the lines were predominantly optically thin by checking that the fluxes of lines from the same upper level were proportional to the ratio of transition probabilities of the lines. Lines were assumed to be unreddened. Excitation temperatures were derived by the procedure adopted by Pandey, Rao & Lambert (1996) for MV Sgr: a quantity F is derived from the line fluxes, where

$$F = \log[W_\lambda F_c(\lambda)] - \log(gf\lambda^3) \qquad (2)$$

W_λ is the equivalent width of an emission line and $F_c(\lambda)$ is the flux in the continuum at the wavelength λ of the emission line. A

Boltzmann plot of $\log F$ against excitation potential of the upper level of the transition χ_u has a slope that provides the reciprocal temperature $\theta = 5040/T$, where T is the excitation temperature. Sample Boltzmann plots are shown in Figs 16 and 17.

The striking result is that the excitation temperatures appear to be roughly constant over the several months spanned by the observations. Component 2, the dominant one, has an excitation temperature near 4000 K throughout the minimum. Component 3 may be systematically slightly cooler. Component 1, which is detectable in few lines, has a temperature close to that of C2. The fact that lines spanning several eV in excitation energy and from three species define a single excitation temperature shows that this
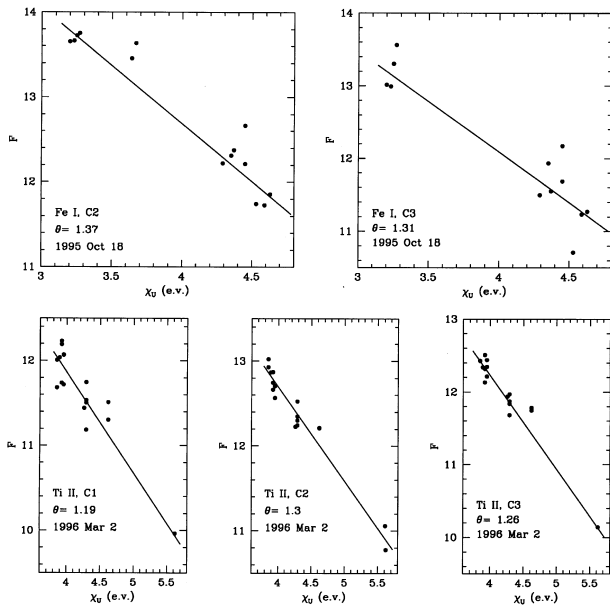
Figure 16. Boltzmann plots for Fe I C2 and C3 components on 1995 October 18, and Ti II C1, C2 and C3 components on 1996 March 2.
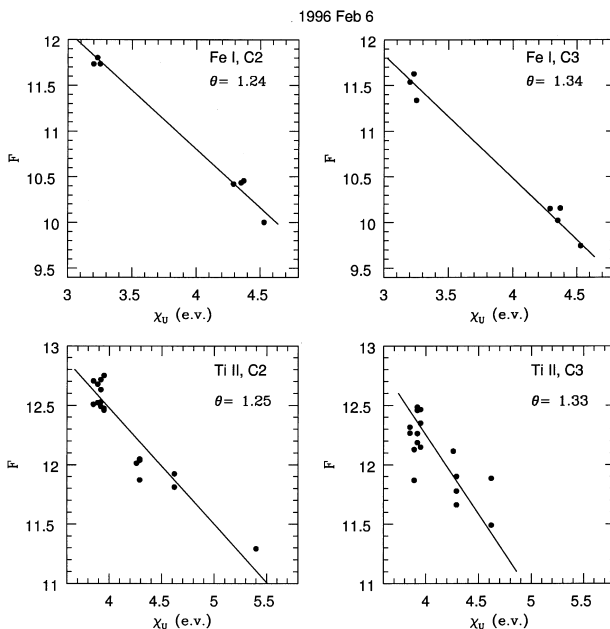
Figure 17. Boltzmann plots for 1996 February 6 for the C2 and C3 components of Fe I and Ti II lines.

temperature is probably close to the kinetic temperature at a value confirmed by the [C I] line ratio and in fair agreement with that inferred from the [O I] lines.

Knowledge of the excitation temperatures enables the ratio of neutral and ionized iron densities to be estimated: e.g. $Fe^+/Fe = 10^{3.3}$ and $10^{3.5}$ for components C2 and C3 on 1996 February 6. There is essentially no change in these ratios over the duration of the decline. Application of Saha's equation of ionization equilibrium to iron on the assumption that ionization and excitation are described by the same temperature gives $n_e \simeq 3 \times 10^7$ cm^{-3} to within a factor of a few. This range includes the n_e estimate from the forbidden lines. An estimate of the total pressure is obtainable from an application of Saha's equation to the ionization of carbon and the assumption that C/He = 1 per cent: the gas pressure is approximately 0.03 dyn cm^{-2} and the gas density is about 2×10^{-9} g cm^{-3}. These estimates are slight underestimates if partial ionization of carbon is suppressed and electrons are contributed by abundant metals. Extrapolated as an isothermal atmosphere, extension of the photosphere corresponding to $\log g = 0.5$ (Asplund et al. 1999) reaches the above gas pressure and density at about 10 scaleheights or a mere $0.04 R_*$ above the photosphere, where the gas pressure is about 500 dyn cm^{-2} at Rosseland mean optical depth $\tau_R \simeq 0.1$ (Asplund et al. 1997) and R_* is the stellar radius. Even if carbon is fully singly ionized, the inferred height corresponds to only $0.05 R_*$. Payne-Gaposchkin (1963) had earlier noted that the temperatures of the emitting region were a little cooler than the stellar temperature but the pressures were markedly less than photospheric values. [Clayton et al. (1992) claim a T of about 6000 K and n_e of about 2×10^{10} cm^{-3} for V854 Cen. The temperature is consistent with ours, but our above-estimated n_e is substantially smaller. These estimates are derived from a set of lines that we would expect are a mix of sharp and broad lines. It is not clear what T and n_e mean when sharp and broad lines are mixed up.] The observation that the sharp lines are not fully eclipsed by the fresh soot cloud, and the size estimates from the [Fe II]/Fe II flux ratios and from the absolute fluxes (see below) show that the emitting region cannot be right above the photosphere. Two interesting questions are obvious. Where around R CrB can one expect emitting gas at a relatively high pressure? Why are the regions immediately above the photosphere not seen in the spectrum?

An estimate of the radial distance is possible from the ratio of forbidden and permitted Fe II lines. Viotti (1976) predicted the flux ratio of 4244-Å [Fe II] to 4233-Å Fe II. Essential radiative and collisional processes were included in the statistical equilibrium calculations. Undoubtedly, better atomic data are now available, but these predictions may suffice to indicate the approximate distance for the region of formation. Viotti assumes that the region is irradiated by a photosphere at 10 000 K, a higher temperature than is appropriate for R CrB. The fact that the line fluxes and the continuum fading are nearly decoupled suggests that either the region is irradiated by the unobscured star throughout the decline, or the excitation of the lines is not dependent on the receipt of photospheric radiation.

Viotti predicts the flux ratio as a function of the dilution factor W and the customary variable $n_e T^{-0.5}$. The observed ratios (see above) run from about 0.008 on 1995 October 18 to 0.13 and 0.45 on 1995 November 13 and 1996 February 6. For the appropriate values of $n_e T^{-0.5} \sim 10^6$, the flux ratio is a simple function of the dilution factor, and hence of the distance of the region of line formation in terms of the stellar radius. The observed flux ratios

imply distances of 2, 18 and 35 stellar radii for the three dates in question. The first estimate is probably erroneous as the Fe II line is expected to be a blend of a sharp and a transient line. The other estimate indicate that the region of formation of the sharp lines is distant from the star, a result consistent with their flux being unaffected by the decline until a considerable fading had occurred.

An estimate of the volume from which sharp lines are emitted may be obtained from the emission-line fluxes. We use the [O I] lines for this purpose, as their excitation is surely by electron collisions and oxygen is expected to be neutral. If the small amount of interstellar and circumstellar extinction is neglected, the equivalent radius of the emitting volume is given by

$$\left(\frac{R_{\rm sh}}{R_*}\right)^3 = \frac{3f_\lambda d^2}{n({\rm O\,I})n_{\rm e}\epsilon} \frac{1}{R_*^3}, \tag{3}$$

where R_* is the radius of the star, f_λ is the integrated line flux, ϵ is the emission coefficient per neutral atom and per electron, d is the distance of the star, and $n({\rm O\,I})$ is the density of oxygen atoms. Adopting plausible values ($R_* = 100\,{\rm R}_\odot$, $d = 1.35\,{\rm kpc}$, ϵ from Surendiranath, $T \sim 4000\,{\rm K}$ with $n_\epsilon \simeq 3 \times 10^7\,{\rm cm}^{-3}$, and an O/C abundance ratio of $10^{-0.2}$), we find $R_{\rm sh} \sim 1.4\,R_*$. This assumes that all electrons are contributed from the ionization of carbon for which we assume Saha's equation and local thermodynamic equilibrium. Alternative assumptions such as full ionization of carbon atoms, or no ionization of carbon with electrons donated by metals, do not yield widely different estimates [say, $R_{\rm sh} \sim (0.4–3)R_*$]. It seems clear that the region emitting the sharp lines is quite distant from the star (say, about $20\,R_*$) and therefore very thin; if the region is a spherical shell, its thickness is $t_{\rm sh} \simeq 0.002\,R_*$ for a shell radius of $20\,R_*$. This is consistent with a single-peaked profile for the emission lines: a thick shell would give emission lines that are double-peaked with a separation between the peaks of approximately twice the expansion velocity.

Comparison of the fluxes in the Ca II and [Ca II] lines confirms the electron densities. At low electron densities and low radiation intensity, the number of photons emitted in the infrared triplet lines equals those emitted in the two forbidden lines. On 1996 February 9, a representative date in the deepest part of the decline, the flux in the triplet lines is about an order of magnitude greater than that in the forbidden lines. Since collisional de-excitation of the ^{2}D state, the common level of triplet and forbidden lines, is expected for $n_{\rm e} \sim 10^8\,{\rm cm}^{-3}$, the low relative intensity of the forbidden lines is explained. A puzzle offered by the apparent absence of a sharp emission line in the H and K lines is sketched below.

6   BROAD EMISSION LINES

Discovery of broad lines may be traced back to Herbig (1949) who found He I 3889 Å, Ca II H and K and the Na I D emission lines to be broad (FWHM $\sim 170\,{\rm km\,s}^{-1}$). The presence of the high-excitation He I line in the set of broad lines implies that these lines have a different origin from the sharp emission lines which are all of low excitation (Payne-Gaposchkin 1963).

Our spectra greatly extend the list of broad lines. Permitted lines include the He I 3889-, 5876-, 7065- and 10 830-Å lines, the Na I D lines, the Ca II H and K lines and the infrared triplet lines 8498, 8542 and 8662 Å, and the K I lines at 7664 and 7699 Å. These identifications of He I lines remove all uncertainty about the correct identification of the 3889-Å line (Herbig 1949; Payne-Gaposchkin 1963). Forbidden broad lines include the [N II] lines

at 6548 and 6583 Å, the [O II] lines at 7319–7331 Å, and the [Ca II] lines at 7291 and 7323 Å. Our detection of the [O II] lines implies that Herbig's (1949, 1968) detections of the [O II] 3727-Å doublet at the 1949 and 1968 deep minima refer also to a broad line. Finally, our spectra also suggest that the C_2 Swan and CN Violet system bands are composed of broad lines at minimum light.

6.1   The He I lines

Neutral helium provides three lines from the triplet series: 3889 Å (2s ^{3}S–2p ^{3}P°), 5876 Å (2p ^{3}P°–3d ^{3}D) and 7065 Å (2p ^{3}P°–3s ^{3}S). The triplet 10 830 Å is surely present at minimum light but the observed bandpass did not usually include the line. The line was strongly in emission on 1996 May 8 when 7065 and 5876 Å did not rise above the local continuum but 3889 Å was obviously in emission. Other triplet lines were searched for but not found. Singlet lines (e.g. 5015 Å 2s ^{1}S–3p ^{1}P°), which would be of comparable intensity for a source in thermal equilibrium, are not present. Their absence shows, as expected, that the He I emission lines result largely from over-population of the metastable 2s ^{3}S level. Profiles of the three detected lines on 1996 March 2 are shown in Fig. 18.

Fig. 19 traces the evolution of the 3889-Å line which was seen first (barely!) in emission on 1995 October 18 and reached its maximum equivalent width in the 1996 January 5 spectrum. Spectra taken in decline prior to 1995 October 18 had not included the 3889-Å region, so its first appearance in emission is not known. Emission was present until 1996 May 8 and all signs of emissions had disappeared by 1996 July 8. Unfortunately, none of the several spectra obtained between May and July included this line. Emission at 3889 Å extends from -280 to $+280\,{\rm km\,s}^{-1}$ at the base with perhaps a slight change with line strength. Inspection of Fig. 19 shows that sharp emission lines prominent when the He I emission line was weak do not mar the line profile when it was at its strongest from 1996 January to March. The reason for this is simple and an important clue to the relative locations of the
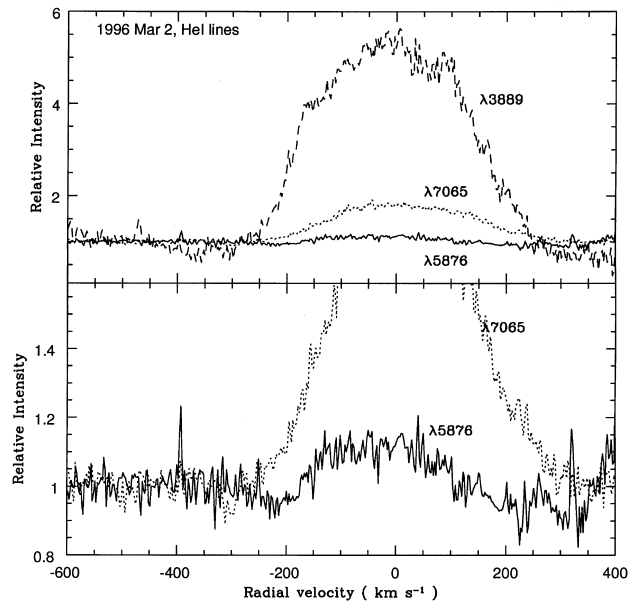
Figure 18. Profiles of three He I lines seen in the 1996 March 2 spectrum. In the top panel, the entire profile is shown. Profiles of the 7065- and 5876-Å lines are shown on an expanded scale in the bottom panel.
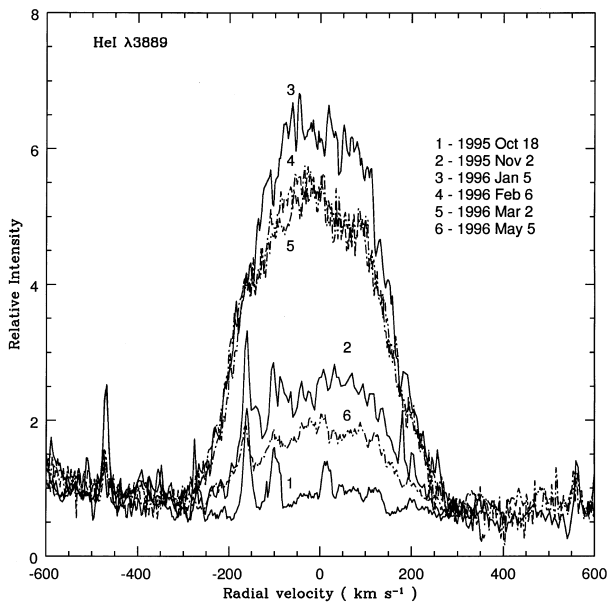
Figure 19. The 3889-Å He I profiles on six occasions – see key. In the early stages of the decline (spectra 1 and 2) and the late stages (spectrum 6), sharp emission lines of Fe I at 3886.3, 3887.0 and 3888.5 Å are also visible.

sharp- and broad-line-emitting gas: the flux of sharp emission lines decreased by a large factor after 1995 November 2, but the broad-line flux was essentially unchanged throughout the decline.

The 5876-Å line is present in absorption at maximum light (Keenan & Greenstein 1963). First appearance of this line in emission occurred on 1996 February 1; it was not present in either absorption or emission on 1995 November 12–15. The line was last seen in emission on 1996 March 13; the next spectrum – 1996 April 9 – again shows neither absorption nor emission. Since the photospheric line is a blend of He I and C I (Lambert & Rao 1994), absence of an absorption implies emission filling in the coincident C I lines (and adjacent lines). Absorption of about the expected strength of the He I–C I blend was present from 1996 May 4 to the end of the series of observations.

The 7065-Å line first appeared in emission above the continuum on 1995 October 18 but was not obviously present on 1995 October 12. It remained as a distinct emission feature until 1996 February 2; the next spectra at 7065 Å from early 1996 May showed very weak emission at the central velocity of the expected broad emission, and hence we suspect that the broad emission at 7065 Å was present. Even this hint of the broad line was absent in 1996 June and on subsequent dates.

The He I emission profiles are well fitted by a Gaussian the width of which (in $km\,s^{-1}$) is the same for the three lines and appears constant over the interval in which the emission lines are prominent. For the well-observed 3889- and 7065-Å lines the mean widths are 322 ± 10 and $323 \pm 22\,km\,s^{-1}$ respectively. The radial velocities of the lines (Table 5) show that the emission at minimum light is systematically blueshifted with respect to the mean photospheric (i.e. systematic) velocity by up to $31\,km\,s^{-1}$. The velocity shift is constant over the period for which the broad lines are measurable. A similar velocity shift is found for the [N II] lines. Unfortunately, the other broad permitted and forbidden lines are too blended for accurate measurement of their velocity.

When emission is strong (1996 February), the 7065-Å line is redshifted by about $3\,km\,s^{-1}$ with respect to the 3889-Å line. This

is at the limit of measurement; the shift is about 1 per cent of the linewidths. The sense of the shift is consistent with the supposition that the 3889-Å and, possibly also, the 7065-Å line are optically thick: we use the wavelength of the strongest component of these $^3S-^3P$ triplets to compute the radial velocities. Since the weakest component of the 3889-Å line is $4.2\,km\,s^{-1}$ to the blue, and is $23\,km\,s^{-1}$ to the red for the 7065-Å line, the effect of optical depth is to introduce a change in the effective wavelengths of the lines.

The fluxes of the He I lines remained constant to within the errors of measurement of about 30 per cent. This is in contrast to the flux of a sharp line which declined by about a factor of 10 between 1995 October 18 and 1996 January and February when the star was at its faintest.

A striking feature of the He I lines is the low intensity of 5876 Å relative to 3889 and 7065 Å. The flux ratios are measured to be $F(7065)/F(5876) \sim 4.8$ and $F(3889)/F(5876) \sim 22$.[4] We may assume that the broad lines are little affected by reddening, and certainly not by the reddening from dust in the cloud responsible for the decline itself. These ratios are quite different from those expected for optically thin lines produced by the recombination of He^+ ions at low density: for example, the prediction is that $F(7065)/F(5876) = 0.12$ and $F(3889)/F(5876) = 0.81$ for gas at $T = 10\,000\,K$ and $n_e = 10^4\,cm^{-3}$ (Aller 1984). The major discrepancy seems to be that the 5876-Å flux is relatively low. Observed and predicted ratios may be reconciled if the lines are optically thick and the electron density is high, permitting collisional excitation: Surendiranath et al.'s (1986) calculations suggest the physical conditions $T \sim 20\,000\,K$ and $n_e \sim 10^{11}$–$10^{12}\,cm^{-3}$. These are quite different from the conditions of the emitting region of the sharp lines.

A remarkable aspect of the He I broad lines is the constancy of their flux. Between the first appearance in mid-October of 1995 and their last appearance in early May of 1996, the flux in the 3889- and in the 7065-Å lines was constant to within 10 per cent, a variation that must equal or even better (!) the measurement errors from the rather indirect calibration of our spectra. The constancy of flux contrasts with the case of the sharp lines, for which the flux in the deepest part of the decline (1996 January–February) fell to 10 per cent of that measured in mid-October of 1995 and out of decline. Our flux estimates for forbidden lines, especially the [N II] 6583-Å line, show that their flux was also constant. This condition likely applies too to the Ca II and Na I D lines, but accurate measurements are compromised by underlying and overlying absorption. This marked difference between the broad and sharp lines shows that their emitting regions are well separated. The broad-line region is not occulted by the fresh cloud of soot. Equally as striking is the fact that the 3889-Å flux is just 24 per cent less than that measured at the time of the 1962 minimum when photographic spectra were calibrated against *UBV* photometry (Rao 1974). Although additional measurements are highly desirable, it appears that the broad-line region is a long-lived feature of R CrB.

6.2 The permitted and forbidden Ca II lines

The Ca^+ ion contributes the 3968- and 3934-Å resonance (H and K) lines, the infrared triplet of lines at 8542, 8662 and 8498 Å, and the forbidden lines at 7291.47 and 7323.89 Å (Risberg 1968). The H and K resonance lines are a transition from the 4s ^{2}S ground

---

[4] Asplund (1995) measured similar flux ratios at the 1993 deep minimum of RY Sgr: F(7065)/F(5876) = 4.3 and F(3889)/F(5876) = 44.

state to the second excited state (4p ^{2}P°), which serves as the upper state of the infrared lines. The lower state of the infrared lines, 3d ^{2}D, and the ground state are connected by the forbidden lines. In optically thin environments, the ratio of the emission coefficients of the H and K lines to the infrared triplet lines is set by a branching ratio favouring the H and K lines. In a low-density gas optically thin to the infrared triplet lines, the number of photons emitted in the infrared triplet lines equals the number emitted in the forbidden lines. In light of these expectations, it is of interest to examine the similarities and differences between the permitted and forbidden Ca II profiles and fluxes.

Broad emission in the H and K lines was seen first on 1995 October 15. On the previous spectrum (1995 October 2) to cover these lines, the lines have essentially their photospheric absorption profile. On the next spectrum – 1995 November 2 – the lines have the basic profile that they retained throughout the decline (Fig. 20): a broad profile with a red peak stronger than the blue peak. Emission was last seen on 1996 May 6 and the photospheric absorption spectrum had returned by 1996 July 8.

Emission in the infrared triplet lines was first seen on 1995 October 13 as *sharp* emission in the 8542-Å line; the other two lines of the triplet were not on the observed portion of the spectrum. The previous spectrum – 1995 October 2 – showed a photospheric absorption line at 8542 Å. The sharp emission in the triplet lines was seen until 1996 July 26 when it was superimposed on a photospheric absorption line. A broad component underlying the sharp feature was seen from 1996 January 5 to March 2.

Emission in the forbidden lines was dominated by a sharp feature, but weak underlying broad emission was seen on 1996 January 5 and February 6. It is likely that this broad emission was present for a longer time but several spectra included not the 7291-Å line but that at 7323 Å the broad emission of which, if present, is masked by stronger broad emission from [O II] lines. The sharp emission line in the [Ca II] lines was seen first on 1995 October 18 and last seen on 1996 March 2. Emission was not present on or before 1995 October 2 and on or after 1996 May 8. The signature
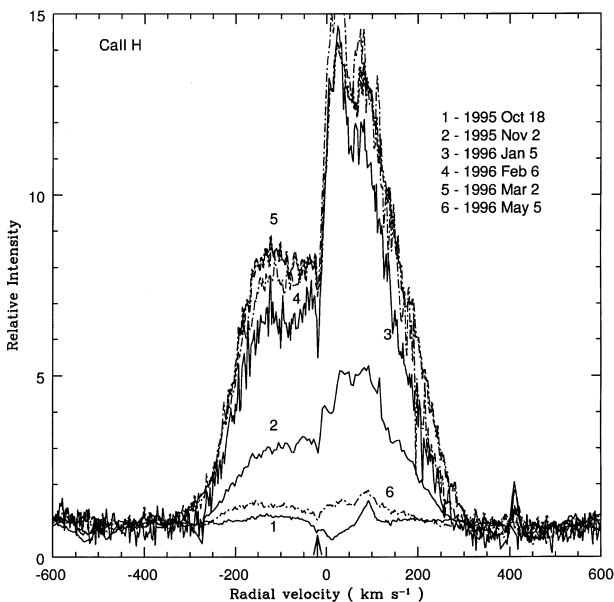
of emission on 1995 October 18 is clear but the spectrum of 1995 November 2 shows no signs of emission.

The flux in the broad infrared triplet lines relative to that in the H and K lines is approximately equal to the branching ratio, and hence the gas emitting the broad lines appears to be optically thin to the H and K lines. The flux in the forbidden lines is about a factor of 10 less than that in the infrared triplet lines, which suggests that collisional de-excitation of the ^{2}D level is occurring, which is expected considering the high densities derived from the He I lines.

The H and K profiles differ from those of He I and [N II]. While the width of the Ca II emission at its base is essentially identical to that of the He I and other broad lines, the H and K lines are distinguished by a marked asymmetry: the red wing is a factor of 2 stronger than the blue wing. This asymmetry is not due to sharp Ca II emission augmenting the red wing. Although interstellar absorption is present at -20 km s^{-1}, it is too narrow to affect the asymmetry of the broad line. We suppose that the asymmetry is caused by absorbing gas at a velocity of -50 to -100 km s^{-1} relative to the systemic velocity of R CrB. This gas, which is not seen in the Na I D profiles, may be gas ejected in earlier declines that is photoionized by the interstellar radiation field and now contains very few neutral sodium atoms.

An intriguing puzzle presented by the H and K profiles is the obvious lack of a contribution from a sharp emission line. If the gas were optically thin to these lines, the flux of the infrared triplet lines would imply a flux in the H and K lines that was about five times the observed flux in the broad H and K lines, but Fig. 20 shows that the sharp-line emission, if present at all, is a small fraction of the broad-line flux. High optical depth in the H and K lines through the sharp-line-emitting region may account in part for this puzzle.
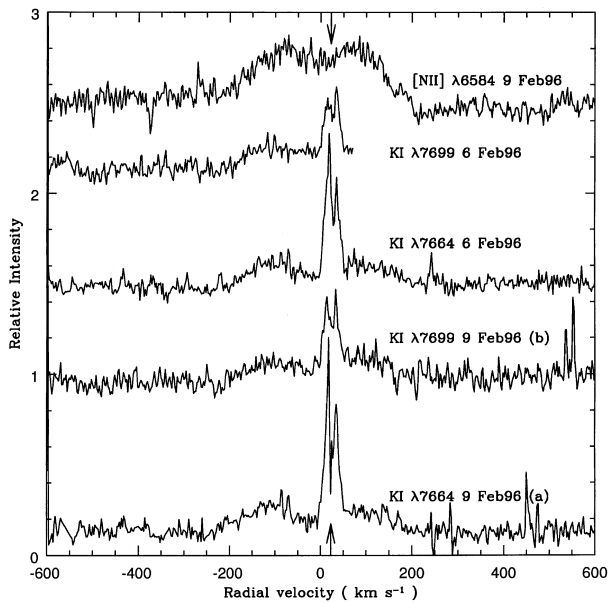
6.3 The K I resonance lines

The K I resonance lines at 7664 and 7699 Å are present as a composite of sharp and broad lines.[5] The broad K I and [N II] lines have similar profiles (Fig. 21). The velocity shift between the broad emission lines and the sharp lines is obvious. The K I sharp line corresponds to components C2 and C3 with no more than a slight contribution from the C1 component. The C2 components of the sharp lines and probably also the broad emission lines are in the intensity ratio of 2 to 1 for the 7664- and 7699-Å, lines indicating that the emitting regions are optically thin to these lines. The C3 component appears to come from somewhat optically thick gas because the intensity ratio is closer to 1:1 than 2:1.
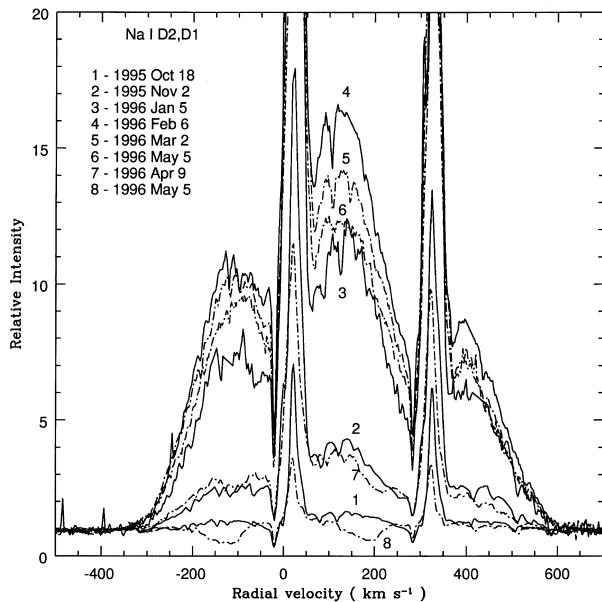
6.4 The Na I D lines

The Na I D lines are the strongest features in the visual region of the R CrB spectrum in decline. Fig. 22 shows representative profiles which are a composite of sharp and broad emission lines with sharp interstellar absorption, and, in the recovery from minimum light, a high-velocity (blueshifted) absorption line. The

Figure 20. Evolution of the Ca II H emission line showing the asymmetric broad line and the narrow interstellar absorption at -20 km s^{-1} denoted by the arrow.

1 - 1995 Oct 18
2 - 1995 Nov 2
3 - 1996 Jan 5
4 - 1996 Feb 6
5 - 1996 Mar 2
6 - 1996 May 5

---

[5] Telluric O_2 crosses this wavelength region. Division of the R CrB spectrum by that of a hot star observed at a similar airmass provides an O_2-free spectrum. Owing to a small instrumental shift, the division produces sharp inverse P Cygni profiles at the wavelengths of the O_2 lines. Such a profile mars the K I 7664-Å line.
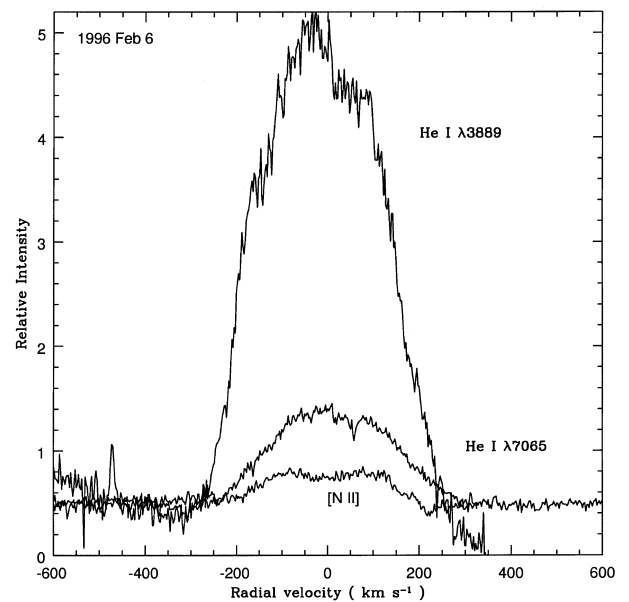
Figure 21. Profiles of the K I resonance lines at 7664 and 7699 Å from 1996 February 6. These consist of a sharp double-peaked emission line and a broad emission line, also double-peaked. The [N II] broad emission line is shown for comparison. The K I spectra have been ratioed to the spectrum of a hot star to remove the telluric O_2 lines. The arrow at $22.5\,\mathrm{km\,s^{-1}}$ indicates the mean photospheric velocity of R CrB.

Figure 23. Line profiles of [N II] 6583 Å, He I 7065 Å and He I 3889 Å from the spectrum of 1996 February 6.

the broad D_1 and D_2 lines. Despite the blending, it is clear that the velocity width of the Na I D lines is quite similar to that of all other broad lines. The sharp Na I D component has contributions from C1, C2 and C3 at all times.

6.5   The [N II] lines

Our spectra provide clear detections of the [N II] 6583-Å line. The accompanying weaker line at 6548 Å is present with the expected lower intensity set by the branching ratio. The excited forbidden line at 5754 Å was never detected. The 6548-Å line was first seen on 1995 November 2 but was not present on 1995 October 18. Emission was seen through to 1996 March 2 but not on 1996 April 9. When the line was detected with good signal-to-noise ratio, the profile was clearly double-peaked (Fig. 23).

The mean velocity separation of the two peaks is $124 \pm 19\,\mathrm{km\,s^{-1}}$ with no evidence of a change during the period of the observations. If treated as overlapping Gaussian profiles, the blue component is found to be possibly slightly broader than the red one ($195 \pm 65\,\mathrm{km\,s^{-1}}$ versus $163 \pm 37\,\mathrm{km\,s^{-1}}$ for the FWHM). The FWHM of the complete line is $279 \pm 35\,\mathrm{km\,s^{-1}}$ from 12 observations, and does not change during the decline. The [N II] line is systematically blueshifted with respect to the photospheric velocity and also with respect to the sharp lines.

There are small but distinct differences between the [N II] and He I emission lines: the [N II] line is double-peaked but the He I lines are symmetrical, and the He I lines are systematically broader by about $40\,\mathrm{km\,s^{-1}}$. The fact that the velocity offset from the photospheric lines is large and similar for all these broad lines suggests that their regions of line formation are related.

A rough estimate of the volume emitting the broad [N II] lines is obtainable by using the lower limit to the flux ratio of the 6583- and 5755-Å lines. The analogous flux ratio of [O II] lines (see below) involves the 7320–7330 Å blend and 3727–3729 Å. Both lower limits imply $n_e \sim 10^6\,\mathrm{cm^{-3}}$ at $T \sim 5000\,\mathrm{K}$. Surendiranath's emission coefficients with the assumptions used for the calculation of the sharp-line region imply a radius of the broad-line

Figure 22. Profiles of the Na I D_1 and D_2 lines from early in the decline to late in the recovery. All spectra are normalized to the local continuum. The velocity scale is set for the D_2 line. On this scale the sharp emission in D_1 appears at about $320\,\mathrm{km\,s^{-1}}$. Interstellar/circumstellar absorption is seen just to the blue of the sharp emission line. Narrow absorption lines at other velocities are telluric H_2O lines.

K I and Na I profiles are quite similar; the higher abundance of Na is presumably responsible for the appearance of absorption components in the Na I D but not the K I lines. A problem peculiar to Na I D is that the smaller separation between the two resonance lines (6 Å versus 35 Å for K I) results in a blending of

region $R_{bl} \sim 6 R_*$. Unfortunately, neither T nor n_e is well constrained. A higher n_e is possible with a contraction of the emitting volume scaling approximately as n_e^{-2}.

6.6   The [O II] lines

Broad emission near 7330 Å is primarily due to [O II] with a minor contribution from the [Ca II] 7323-Å line (Fig. 11). The shape of the emission indicates that it is a blend of the four expected [O II] lines: 7319.99 Å ($^2D_{5/2} - {}^2P_{3/2}$) and 7318.92 Å ($^2D_{5/2} - {}^2P_{1/2}$) providing 'one' line and 7330.73 Å ($^2D_{3/2} - {}^2P_{3/2}$) and 7329.66 Å ($^2D_{3/2} - {}^2P_{1/2}$) providing the second 'line'. (Wavelengths are taken from Moore 1993.) These two 'lines' are blended into one asymmetric broad line. The shape of the profile suggests that the dominant contribution is made by the pair of lines (7319.99 and 7330.73 Å) from the $^2P_{3/2}$ upper state, as expected. No attempt has been made to deconvolve the line into its one [Ca II] and four [O II] components. The linewidth is quite consistent with those measured for the [N II] 6583-Å line. Unfortunately, the [O II] 3727-Å doublet was never recorded with adequate signal-to-noise ratio.

6.7   Molecular emission features

C$_2$. Absorption bands of the C_2 Swan system are weakly present in the spectrum of R CrB at maximum light with a variable strength. At the onset of the decline, the C_2 lines go into emission: Fig. 24 shows the 5165-Å bandhead in emission on 1995 October 18 when transient emission lines were strong. Emission had weakened by 1995 November 2 when the presence of C_2 in absorption or emission is difficult to establish. The next observation covering the 0–0 band shows it to be in emission (Fig. 24). Even casual inspection of Fig. 24 shows that the C_2 lines are not sharp on 1996 January 5. If they were, the emission spectrum would be the inverse of the normal absorption spectrum with probably less mutilation by atomic lines. Striking features of the emission

Figure 24. Spectra of the C_2 0–0 P-branch bandhead on 1995 October 18, 1995 November 2 and 1996 January 6. Note the bandhead in emission on 1995 October 18, and displaced to shorter wavelengths on 1996 January 6.

spectrum are that the head is missing, the rotational structure is unresolved, and the peak intensity is displaced from 5165 Å, the wavelength of the head in absorption, to about 5162 Å. A quite similar band profile was present at a minimum of V854 Cen (Rao & Lambert 1993) and attributed to C_2 line formation in cold gas: P-branch lines of low rotational quantum number have wavelengths near 5162 Å. The linewidth suggests that the regions responsible for the broad C_2 and the various atomic broad lines may be related but, in view of the different physical conditions required for C_2 and He I emission, the regions cannot be co-located. The C_2 emission consists of many blended lines, so that it is not a simple matter to derive the radial velocity of the molecular gas. The great width of the C_2 lines may indicate motion – turbulent or organized – of the gas, or it may arise because the emitting molecules are between us and the scattering layer that is presumed to broaden the photospheric lines (see below).

A search was made for lines of the C_2 Philips bands. The lower electronic level for the Philips system is the ground state of the molecule. The lower level of the Swan system is the lowest triplet level lying slightly above the ground (singlet) level. A combination of observations of Swan and Phillips bands would provide data on the excitation of the molecule, and hence clues to the location of the molecular gas. Our search for Phillips lines provided nothing more than tantalizing hints of absorption and emission lines. We postpone further discussion pending a full search for 2–0 and 3–0 lines which fall in regions containing telluric lines.

CN. The $\Delta v = 0$ sequence of CN violet system bands was seen in emission first by Herbig (1949) when R CrB was in a deep decline ($V \sim 14$). Additional observations were reported by Payne-Gaposchkin (1963) and Herbig (1968). In our observations, the $\Delta v = 0$ sequence is first seen in emission on 1995 October 18 with a rotational structure suggesting that the individual CN lines are sharp. At the next observation of the sequence on 1996 February 6, the appearance of the band has changed dramatically: individual lines are no longer resolved and the bandhead has shifted to the blue. At this time, the CN and C_2 bands have similar appearance. The blueshifting of the CN band in decline was noted by Herbig (1949).

7   HIGH-VELOCITY ABSORPTION LINES

A striking feature of the Na I D profiles at earlier declines has been the appearance of a strong broad blueshifted absorption. This decline was no exception: Fig. 22 shows such absorption in the 1996 May 5 spectrum. Blueshifted absorption was noted first by Payne-Gaposchkin (1963) in spectra taken during recovery from the 1960 minimum. It was seen again in the recovery from the 1988 minimum (Cottrell et al. 1990; Lambert et al. 1990). Clayton (1996) remarks that high-velocity absorption lines have been seen 'early in declines and again just before return to maximum light'. No absorption was seen early in this decline. A similar statement applies to the 1988–89 decline when high-velocity absorption was seen clearly first at 100 d after the onset, and possibly at a lower velocity at 80 d after the onset. At these times R CrB was at a visual magnitude of about 10 which it had reached about 30 d into the decline.

In this minimum, we first detect high-velocity absorption in the 1996 April 9 spectrum when the star was at $V = 12.2$ and recovering from minimum light. Comparison of Na I D profiles obtained at the same visual magnitude in the descent to and
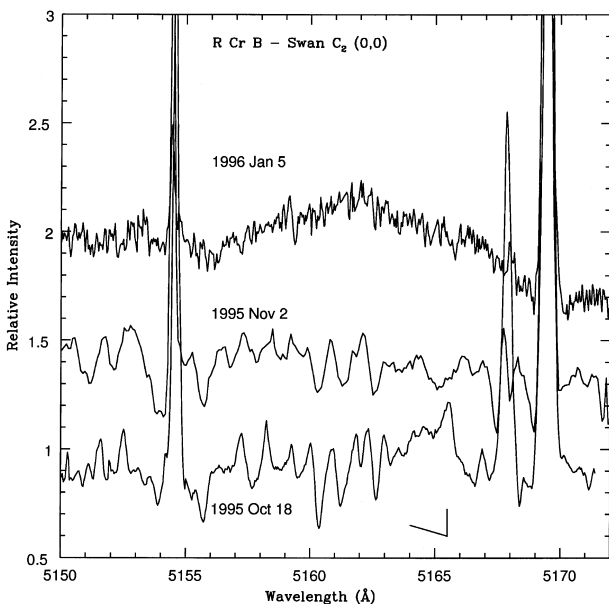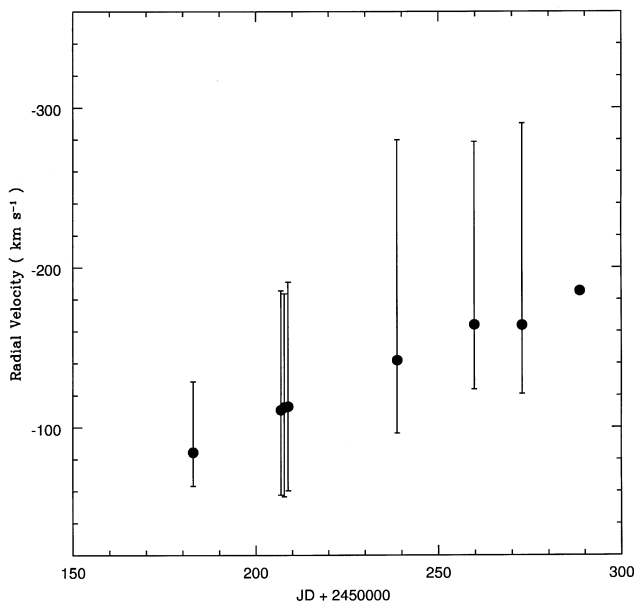
Figure 25. Evolution of the Na I D shell absorption velocity. The velocity of the deepest part of the absorption is shown by the filled circles with the vertical bars denoting the extent of absorption. For the final point in the sequence the extent is not shown because the absorption had broken into several distinct components.

recovery from minimum light (spectra 2 and 7 in Fig. 22) shows that the broad emission profiles of Na I D are essentially identical except for the weak shell absorption in the spectrum taken on the recovery. As the recovery progressed, the shell absorption changed: the equivalent width of D_1 increased from 0.078 Å on 1996 April 9 to 0.73 Å on May 5 as the mean velocity changed from -85 to $-113 \,\mathrm{km\,s^{-1}}$. The profile is asymmetric with the red wing steeper than the extended blue wing. The velocity of the deepest part of the profile increases from $-85 \,\mathrm{km\,s^{-1}}$ on 1996 April 9 to $-190 \,\mathrm{km\,s^{-1}}$ on July 25 (Fig. 25). In late 1996 July, the profile split into several components. By 1996 October 2, the shell absorption had disappeared.

Shell absorption is not present in the Ca II H and K lines. Superposition of Na I D and Ca II profiles shows quite clearly that shell absorption is absent in the latter profile. There is a hint of shell absorption in the best K I profiles.

Although reports of shell absorption are scarce, the above evolution appears typical. Certainly, the maximum velocity in the 1988–89 decline and the present decline are similar. In the former decline, maximum velocity was attained in just 100 d from onset of the decline instead of the nearly 300 d taken in the recent decline, which may reflect the fact that the 1988–89 decline was shallower (minimum $V = 11.2$ against 13.6). Payne-Gaposchkin (1963) reported a velocity of $-275 \,\mathrm{km\,s^{-1}}$ for shell absorption from the 1960 minimum. This is appreciably higher than we find. She also reported shell absorption in the Ca II H and K lines which the recent decline did not show. The sparse data set encourages the view that shell absorption appears only during the recovery from minimum light. Extrapolation of the velocity of the maximum absorption and the extrema of the absorption (Fig. 25) implies that the acceleration of the shell began in early 1996 January, close to the mid-point of the 150-d interval at minimum light. In the case of stars exhibiting frequent declines (e.g. V854 Cen), shell absorption may appear at other phases because it may be difficult to tie the shell absorption to the responsible decline. Additionally,

shell lines may be present and lack an associated decline; gas from clouds off the line of sight may intrude on to our line of sight.

8 PHOTOSPHERIC LINES AT MINIMUM LIGHT

Soot formation above the photosphere is considered to be the agent responsible for the decline. As discussed above, the trigger for soot formation appears to be seated in the photosphere. Here, we investigate if the decline leaves a mark on the photosphere in the form of a change of chemical composition which we determine for several dates during the decline, excluding the times when the star was at its faintest. This exclusion is necessary because the absorption-line spectrum is then 'veiled', i.e. the lines are shallow and very broad. Discussion of the chemical composition is followed by remarks on the veiled photospheric lines.

8.1 Chemical composition

Spectra from the following four epochs were selected for measurement:

(i) 1995 September 30 – the decline began at about this time;
(ii) 1995 October 18 – the star had faded to $V \simeq 10$;
(iii) 1995 November 2 – the decline of the brightness of the star had continued and the star was close to $V \simeq 12$ at this time;
(iv) 1996 May 5 – recovery was underway with the star at $V \simeq 10.4$.

This quartet of spectra were compared with that obtained prior to the decline on 1994 April 2 when the star was close to maximum light in its pulsational cycle (Rao & Lambert 1997). Comparison of the measured equivalent widths shows that the lines in the 1995 September 30 spectrum are up to a factor of 2 stronger than in the pre-decline maximum light spectrum. At the other three epochs, the equivalent widths are quite similar to the pre-decline case.

Our method of analysis follows that developed for the comprehensive abundance analysis of RCB stars (Asplund et al. 1999; see also Rao & Lambert 1996). We use the line-blanketed H-poor atmospheres computed by Asplund et al. (1997). An abundance ratio C/He = 1 per cent by number is adopted. The microturbulence is derived from Fe I and C I lines by the usual condition that the derived abundance be independent of the equivalent width. A selection of Fe I and Fe II lines and the condition of ionization equilibrium are used to fix the atmospheric parameters T_{eff} and $\log g$. As an additional constraint on T_{eff} in three of the five cases, we use the low-excitation [O I] 6363-Å line and high-excitation permitted O I lines. The parameters $T_{\mathrm{eff}} = 6700 \,\mathrm{K}$, $\log g = 0.0$ and the microturbulence of $7 \,\mathrm{km\,s^{-1}}$ fit the selected indicators. That a single model suffices is not surprising because Rao & Lambert (1997) showed that the atmospheric pulsation results in only small variations of the parameters.

Results for the abundances are summarized in Table 6. There is a suggestion that the abundances derived from the 1995 September 30 data are consistently higher than at other times by about 0.3 to 0.5 dex. Relative abundances X/Fe are, however, almost identical for this and other spectra. It is likely that the apparent difference in composition reflects the atmospheric disturbance that subsequently initiated the decline. Since such a disturbance is not modelled by the adopted suite of model

Table 6. Chemical composition before and during the decline.

Species	1994 Apr 2 $\log \epsilon^a$	1995 Sep 30 $\log \epsilon$	Δ^b	1995 Oct 18 $\log \epsilon$	Δ	1995 Nov 2 $\log \epsilon$	Δ	1996 May 5 $\log \epsilon$	Δ
H I	6.91	7.02	-0.3	6.48	-0.3	6.38	-0.3	7.05	0.2
Li I	2.42	2.93	0.1	...	...	2.33	0.1	...	...
C I	8.92	9.31	0.0	...	...	8.81	0.1	8.99	0.1
C II	...	...	...	9.23	...	...	...	...	...
N I	8.13	8.40	-0.1	7.66	-0.3	7.91	0.0	7.80	-0.3
[O I]	8.46	8.91	0.1	...	...	...	...	8.67	0.3
O I	8.39	8.94	0.2	8.26	0.0	8.40	0.2	8.76	0.4
Na I	6.17	6.66	0.1	5.72	-0.3	5.85	-0.1	6.27	0.2
Mg I	6.87	7.38	0.1	...	...	6.81	0.1	7.10	0.2
Mg II	...	...	...	...	...	6.49	...	6.75	...
Al I	5.75	5.99	-0.1	...	...	5.65	0.1	5.70	0.0
Al II	...	...	...	5.81		...	...	6.10	...
Si I	7.03	7.08	-0.3	6.47	-0.4	6.69	-0.2	6.85	-0.1
Si II	7.18	...	...	...	...	6.85	...	7.14	...
S I	6.57	6.90	-0.1	6.35	-0.1	6.56	0.2	6.69	0.2
Ca I	5.23	5.58	0.0	...	...	5.15	0.1	4.77	-0.4
Fe I	6.32	6.71	...	...	...	6.14	...	6.14	...
Fe II	6.26	6.63	...	6.13	...	6.06	...	6.23	...
Ni I	5.46	5.82	0.0	...	...	5.31	0.0	5.62	0.2
Zn I	3.81	4.36	0.2	3.56	-0.1	3.73	0.1	4.17	0.4
Y II	1.42	1.79	0.0	...	...	...	...	...	...

^{a} Normalized such that $\log \Sigma_{\mu_i n_i} = 12.15$ where μ_i is the atomic weight.
$^b \Delta = [\text{X/Fe}] - [\text{X/Fe}]_{1994 \ \text{Apr2}}$ where $[\text{X/Fe}] = \log(\epsilon_X/\epsilon_{Fe})_{R \ CrB} - \log(\epsilon_X/\epsilon_{Fe})$.

atmospheres, the result is the apparently anomalous abundances. Perhaps significantly, the carbon abundance derived from the 1995 September 30 spectrum is much closer to the adopted input abundance than is the case for the other spectra. In fact, the derived and input abundances are identical to within the errors of measurement: Table 6 gives the derived abundance as 9.3 ± 0.3 and the input value is 9.5. At other times, the derived carbon abundance is 0.5 to 0.7 dex less than the input value. Since carbon dominates the continuous opacity, the equivalent width of (weak) C I lines should be independent of the abundance. Asplund et al. (1999) dub the inconsistency between the derived and input carbon abundances 'the carbon problem'. After consideration of possible resolutions of the problem, they conclude that the key lies in the atmospheric structure. It may then be significant that, at the time when the photosphere is disturbed, the carbon problem is considerably mitigated.

If the ratio X/Fe is taken as a more secure estimator of chemical composition, it may be claimed that the photospheric composition is unaffected by the decline. This is most probably not unexpected. There are, however, examples of luminous supergiants with highly peculiar compositions resulting from the efficient separation of elements according to their condensation temperature. For example, certain RV Tauri variables are highly deficient in Ca, Fe and Sc but not in S and Zn (Giridhar, Lambert & Gonzalez 1998). Many of these stars have dusty wind and/or circumbinary discs in which a separation of dust from gas may occur. If such a separation and return of (dust-free) gas to the atmosphere can occur for RV Tauri stars, might it not occur for R CrB? The lack of change in the X/Fe ratios, as signified by the quantity Δ in Table 6, suggests that it did not occur at the 1995–96 decline. Of course, the abundance anomalies resulting from a dust–gas separation may differ considerably for RV Tauri and R CrB, owing to the large difference in chemical compositions, and in pulsational amplitudes which are considerably larger for the RV Tauri variables. In addition, the presence of high-velocity absorption in Na I D lines shows that at least some metals are in the gas that is ejected with the dust. Sodium, however, has a relatively low condensation temperature. Calcium has a much higher condensation temperature, so that it is intriguing that high-velocity absorption was not seen at this decline in the Ca II H and K lines.

8.2 Profiles of absorption lines

Previous reports of the spectra of RCBs in deep declines have noted the weakness of the photospheric absorption lines. Adjectives 'veiled' and 'diluted' have been applied to describe the appearance of the lines. High-resolution spectra of V854 Cen in a deep decline showed the lines to be absent even though the continuum was recorded at a signal-to-noise ratio more than adequate to detect all but the weakest lines (Rao & Lambert 1993). Our spectra betray the evolution of the absorption-line spectrum from a normal photospheric spectrum to a veiled spectrum at minimum light. (In the early stages of the decline, some high-excitation lines are filled in by emission. The apparent disappearance of these absorption lines is not an example of veiling.)

Low-excitation lines at minimum are irretrievably blended with their own sharp emission line. To study the evolution of absorption lines we therefore consider high-excitation lines that, after the disappearance of their transient emission lines, return on 1995 November 2 to their pre-decline profile and equivalent width. On the next spectrum (1995 November 12), these strong lines appear greatly weakened. A superior spectrum from 1996 January 5 shows the lines weakened, broadened and redshifted (Fig. 26). These are 'veiled' lines which at this decline were present when the star was fainter than $V \simeq 12.5$. Table 7 summarizes measurements of a set of strong lines. The normal absorption lines return by 1996 May 5.

9 NEW INSIGHTS FROM SPECTROSCOPY OF THE 1995–96 DECLINE

Spectroscopy of the 1995–96 decline provides detailed evidence

Table 7. Strong absorption lines in and out of decline.

| Line | Maximum light[a] | | | | In Decline | | | | | | | | |
| | 1994 Apr 2 | | 1994 Apr 29 | | 1995 Nov 2 | | | 1996 Jan 5 | | | 1996 Feb 6–9 | | |
	W_λ[b]	HW[c]	W_λ	HW	W_λ	HW	ΔV[d]	W_λ	HW	ΔV	W_λ	HW	ΔV
O I 6158 Å	365	40	343	40	356	40	−8	188	…	11	…	…	10
Si II 6347 Å	594	43	527	43	552	44	−11	265	67	15	234	63	13
Si II 6371 Å	469	34	374	34	471	39	−10	269	81	11	139	52	7
H I 6563 Å	547	52	497	52	425	…	−5	220	69	10	…	…	12
S I 6743 Å	130	27	149	27	130	26	−12	…	40	…	…	53	13
S I 6749 Å	184	28	178	28	160	27	−11	…	…	17	81	…	5
S I 6757 Å	192	28	196	28	197	29	−11	…	40	…	96	75	…

| Line | In Decline | | | | | | | | |
| | 1996 Mar 2 | | | 1996 Apr 9 | | | 1996 May 5 | | |
	W_λ	HW	ΔV	W_λ	HW	ΔV	W_λ	HW	ΔV
O I 6158 Å	248	…	11	280	…	6	383	45	8
Si II 6347 Å	…	…	…	392	46	16	…	…	…
Si II 6371 Å	243	64	10	276	35	7	479	40	8
H I 6563 Å	…	…	8	…	…	9	523	49	7
S I 6743 Å	69	36	9	116	32	9	157	33	4
S I 6749 Å	84	37	…	136	31	6	201	32	6
S I 6757 Å	130	46	9	…	…	…	224	…	5

[a] Measurements from Rao & Lambert (1997) to show approximate range.
[b] Equivalent width in mÅ.
[c] Full width at half-maximum line depth in $km\,s^{-1}$.

on R CrB and its environs which we now endeavour to relate to the generic model that envisages a fresh localized cloud of soot forming and obscuring the photosphere. Five principal spectroscopic components and/or events should be noted. First, there is the photospheric disturbance occurring at the onset, an event we refer to as the 'trigger', which provided distorted absorption-line profiles and transient emission lines. Secondly, there are the many sharp emission lines of neutral and singly ionized metals which appear largely unaffected by the decline. Thirdly, there are the broad emission lines of He I and other species. Fourthly, there is a veiling of the photospheric lines at minimum light. Fifthly, there is the appearance following minimum light of high-velocity blueshifted absorption in the Na I D lines. We discuss each of these aspects.

9.1 The photospheric perturbation and transient emission lines

Spectra taken at the onset of the decline show a disturbed photosphere with upper layers falling down and the deepest layers moving up at a velocity greater than that expected from the extrapolation of the previously regular pulsation. The photometric decline appears to have occurred when the photosphere was expected to have its maximum velocity of recession. In a few days following onset, the transient emission lines appear at a velocity close to the mean photospheric velocity. We identify the disturbed absorption lines and transient emission lines as signatures of a shock.

Transient emission lines appear about 2 weeks after the first observations of the distorted photospheric lines, but incipient emission seems to be present somewhat earlier. There must be a physical relation between the affected photospheric absorption lines and the transient emission lines. It seems unlikely that the regions of formation are exactly co-located. A possibility is that the shock to which the photospheric disturbance is attributed migrates outward to initiate emission in lower density regions.

Emission in O I high-excitation lines and in molecular C_2 lines is unlikely to arise from the same layers of the atmosphere. We suppose that the high-excitation emission lines arise from gas heated immediately behind the shock. A possibility suggested by theoretical studies of pulsating R CrB atmospheres is that the low atmosphere contains more than one shock: for example, Woitke (1997) obtains steady-state solutions for a regularly pulsating atmosphere in which a shock propagates outward at each pulsation, but at times two shocks are supported by a pulsation, and the velocity of the principal shock (relative to the star) varies with pulsational phase from about zero to close to the velocity v_1.

In models considered by Woitke (1997; see also Woitke, Goeres & Sedlmayr 1996), emission lines are formed in hot gas immediately behind a shock. Cooling times for the hot gas appear to be very short – less than a day for a typical model (Woitke 1997) – and, therefore, the persistence of the transient emission lines over a couple of weeks implies that shock propagation maintains the emission-line spectrum. Further behind the shock in the expanded gas, densities and temperatures are lowered with the result that cooling times are lengthened. It is in this post-shocked gas that conditions may be conducive to dust formation provided that the gas is sufficiently distant from the star.

Defining the shock velocity v_1 to be that of the pre-shock gas in the reference frame of the shock, Woitke's calculations for a R CrB-like star show that dust may form closer to the star for higher velocities of the outward-moving shock: for example, $v_1 = 50\,km\,s^{-1}$ provides for dust formation as close as $0.5\,R_*$ to the stellar photosphere, but at $v_1 = 20\,km\,s^{-1}$ dust cannot be formed closer than about $3\,R_*$ to the surface. The velocity of the emitting gas relative to the star, v_*, depends on the velocity of the shock through the gas and the velocity of this gas relative to the star. If the atmosphere is static, $v_* \sim v_1$. [Woitke (1997) finds a velocity of $v_* \simeq v_1/2$ for the case of a representative periodic shock.] The observed radial velocity of the emission lines depends on the location and size of the shocked region on the Earth-facing hemisphere. A small region near the centre of the hemisphere will give emission lines at the shock velocity, but lines from an
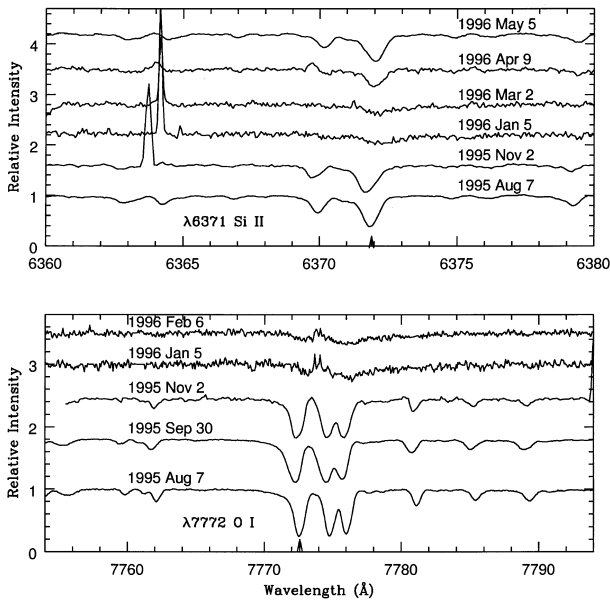
Figure 26. Spectra showing the normally strong Si II 6371-Å line (top panel), and the normally strong O I 7772-Å triplet (lower panel) on several occasions. All spectra are to the same but are displaced in relative intensity for clarity. These lines are weakened, broadened and redshifted on spectra obtained from 1996 January to March.

off-centre region will have a smaller radial velocity which vanishes for a region at the limb. Emission from a large region will have a mean velocity between v_* and zero. If the shock propagates through infalling gas, v_* will be reduced by the infall velocity. In the 1995 decline, there is evidence from the photospheric line profiles at the onset and from the redshifted absorption feature accompanying the transient emission lines that gas was infalling at about $30 \, \mathrm{km \, s^{-1}}$ relative to photospheric lines. This gas may be ahead of the 'dusty' shock or possibly related to a deeper inward-moving shock. The transient emission lines are typically redshifted by about 7 to $17 \, \mathrm{km \, s^{-1}}$ relative to the group A absorption lines, which are blueshifted by about $10 \, \mathrm{km \, s^{-1}}$ relative to the predicted photospheric velocity. These velocities seem to imply passage of a shock through infalling gas.

Observations suggest a casual relation between the appearance of the shock and the onset of the decline. The delay between the occurrence of the shock in the photosphere and the formation of dust higher in the atmosphere appears to have been short. However, the lack of spectra between 1995 August 9 and September 30 means that the birthdate of the photospheric shock is *not* known with precision. The presence of infalling gas prompts speculation that the trigger preceded the decline. Perhaps, the previous pulsation began the sequence of events that led to the decline. If it can be shown that the appearance of the photospheric shock and the onset of the decline are contemporaneous, it seems that two shocks have to be invoked because dust cannot form behind a photospheric shock and that shock will require at least several days to propagate out to the heights at which temperatures in the post-shock gas are sufficiently cool for dust to form. In this case, one might expect to observe different radial velocities for lines formed in the two shocks, and hence different radial velocities for high- and low-excitation lines and evidence of two velocity components in some lines. These effects were not seen.

R CrB is a regular pulsator but declines, apparently shock-initiated, occur at random intervals. This decline occurred at maximum pulsational velocity which seems to be the phase at which RY Sgr (Pugach 1977) and V854 Cen (Lawson et al. 1992) may also go into decline. Evidence of photospheric shocks in the form of line splitting has not been seen in the course of the pulsation, but is seen in RY Sgr (Danziger 1963; Cottrell & Lambert 1982; Lawson 1986; Lawson, Cottrell & Clark 1991; Clayton et al. 1994), a larger amplitude pulsator. One supposes that a pulsation of slightly above average amplitude occurs, leading to the phenomena seen here at the 1995 onset. [RY Sgr, with a larger velocity amplitude pulsation but an otherwise very similar atmosphere, is not more prone than R CrB to declines; and V854 Cen, with a small velocity amplitude, is especially susceptible to go into decline (Lawson & Cottrell 1997).] This scenario may explain the decay of the transient emission lines. Stellar pulsation leads to periodic development and propagation of shocks that prove inadequate for the spawning of dust. An abnormal shock develops, possibly related to an abnormal pulsation, and dust grows in the unusually cool post-shock gas. This shock propagates outwards, spawning dust. Transient emission lines come from lower altitudes primarily where gas densities are higher. At the passage of the next and regular shock, the gas is cycled through the shock, but the post-shock gas is now warmer and unable to sustain dust growth or the flux in the transient emission lines. If the abnormal shock is not repeated, transient emission lines may last no more than about a single pulsational period of 40 d, as is observed. Dust formation continues at higher altitudes as the abnormal shock moves up, and the next normal shock, encountering cooler and dustier gas than usual, may also spawn dust.

If the seat of the trigger is the photosphere and its pulsations, there is the hope that continuous monitoring of R CrB will establish the time delay between a photospheric disturbance and the onset of a photometric decline. Such monitoring would also reveal whether the 1995 decline was typical or not. If the trigger is seated higher in the atmosphere, its first appearance may be unobservable spectroscopically except perhaps in the ultraviolet.

9.2 The broad emission lines: is R CrB a binary?

The broad emission lines betray the presence of hot dense high-velocity gas, the siting of which in the atmosphere of R CrB itself raises many problems. Our alternative site is an accretion disc around a compact companion to the supergiant, i.e. we propose that R CrB is a spectroscopic binary. Our interpretation was suggested in part by the discovery of broad emission lines in the spectrum of the white dwarf Mira B (Joy 1926, 1954). Deutsch (1958) recognized that (H-rich) gas captured from the wind fed by Mira A, the long-period variable, could be responsible for the emission lines. Warner (1972), Livio & Warner (1984) and Reimers & Cassatella (1985) invoked an accretion disc around Mira B as the site of the emission lines.

Introduction of the secondary and its accretion disc solves two principal puzzles presented by the broad lines – what is the excitation source for the He I lines, and why are the lines so broad? The fundamental energy source is the deep gravitational potential well provided by a white dwarf companion; gas flowing through the accretion disc is heated by 'friction'. The width, as we show below, is simply due to the Keplerian velocity of gas in the disc close to the white dwarf. More fundamentally, a realization that R

CrB is a binary with a compact companion suggests that this and some other R CrB stars may be the fruits of stellar evolution of a binary system.

Spectroscopic similarities between the width of the broad emission lines of R CrB and those from Mira B and other systems with accretion discs around white dwarfs provide suggestive but not conclusive proof that R CrB is also accompanied by a disc and a white dwarf. The clearest proof would come from radial velocity variations of R CrB itself and of the broad-line-emitting region.

The broad lines are detectable only when R CrB is about 5 or more magnitudes below maximum light. In the 1995–96 decline the He I lines were detectable with profiles adequately defined for a radial velocity measurement for about 6 months (Table 5). To within the measurement errors, the velocity of the broad lines was constant. The only other measurement of the He I lines appears to be that by Herbig (1949) of the 3889-Å line in 1949 February at a velocity essentially identical to that reported here, which implies either that the observations sampled the radial velocity curve at a similar velocity, or that R CrB is a single star and the He I lines are emitted by gas associated with R CrB itself.

In our search for orbital motion of R CrB, we examined the 149 measurements of radial velocity referred to in Section 3.1. As noted there, the complete set suggests a pulsational period of 42.6968 d or, if the oldest measurements are omitted, a period of 42.7588 d. In either case, there is little evidence for a longer term (i.e. orbital) velocity variation. If R CrB is a spectroscopic binary, the lack of a detectable orbital velocity variation implies that the γ-velocity must be close to the mean velocity of 22 km s^{-1} and the (projected) velocity amplitude of R CrB is less than about 3 km s^{-1}. [A notable oddity is the apparent absence of a pulsational variation in the measurements reported by Fernie et al. (1972). This may be due to an unfortunate distribution of the measurements with respect to phase. These measurements may be fitted by the mean curve if it is displaced about 4 km s^{-1} to higher velocities. Perhaps this displacement is the result of orbital motion.]

If the He I lines are associated with gas moving with the velocity of the secondary, the velocity amplitude of the secondary star is at least 30 km s^{-1}, the velocity difference between the He I lines and the systemic velocity in the 1995–96 decline. These estimates of the velocity amplitudes imply a mass ratio $M_R M_{Sec} \gtrsim 10$ independent of the inclination of the orbit to the line of sight. The orbital period must be sufficiently long that the 6-month-long observations of an essentially constant radial velocity from the He I lines are consistent with the predicted (slow) velocity variation. Although the required period is dependent on the orbital eccentricity, a period longer than about 2 yr would seem to be demanded.

Brightness variations at 3.5 μm were reported by Stecker (1975) to be periodic with a period of 1100 d. This suggestion was reconsidered by Feast et al. (1997) who estimated that the period might be 1260 d. No suggestion was made that such a period was an orbital period. Since the warm infrared-emitting dust is relatively distant from the star, the orbital diameter (see below) may be much smaller (say a few stellar radii) and 'interference' between the infrared flux and the location of the secondary seems unlikely. Optical polarization measurements of R CrB (Stanford et al. 1988; Clayton et al. 1997) indicate a preferred direction for ejection and/or accumulation of dust which conceivably could be an orbital plane; Clayton et al. propose a bipolar geometry.

It is readily shown that a circular orbit corresponding to a period of (say) 1260 d and a mass ratio of 10 corresponds to a separation of the two stars of about 630 R$_\odot$, and maximum radial velocity amplitudes of 2.3 and 23 km s^{-1} for a 2-M$_\odot$ R CrB star and a 0.2-M$_\odot$ companion respectively. The photospheric radius of R CrB is about 100 R$_\odot$, which is substantially smaller that the Roche lobe ($R \simeq 250$–300 R$_\odot$). The secondary, if a compact object, is much smaller than its Roche lobe. These geometrical parameters are not greatly sensitive to the choice of period and mass ratio. In the accretion disc that is fed presumably by the wind of R CrB, Keplerian velocities of 200 km s^{-1} are attained at about 0.5 R$_\odot$ from the secondary. The observed velocities are dependent on the angle of inclination to the line of sight. The broad optically thick He I lines are presumed to be emitted by these inner regions of the disc. The broad forbidden lines are emitted by a much more extended region, say $R_{bl} \sim 6R_* \simeq 600$ R$_\odot$ if $n_e \sim 10^7$ cm^{-3}. In order for the broad forbidden lines to reflect, as we assume, the orbital motion of the secondary, their emitting volume must be approximately centred on the secondary with a radius less than the separation between the two stars. This separation is about $6R_*$. With a slight increase in the assumed n_e, R_{bl} can be made less than this separation.

The binary scenario makes qualitative sense geometrically. The least satisfactory aspect of the scenario concerns the stellar masses inferred from the lower limit to the mass ratio, an observational limit that is not dependent on the assumed orbital inclination. A mass of 2 M$_\odot$ for R CrB is about the maximum conceivable given the space distribution of these stars. At first glance, a white dwarf mass of less than 0.2 M$_\odot$ seems hardly credible. A lower mass for R CrB, say 1 M$_\odot$, implies a lower mass for the white dwarf, say 0.1 M$_\odot$. A mass of 0.1–0.2 M$_\odot$ for a white dwarf is less than the average mass of a white dwarf in the field or in a cataclysmic binary (Warner 1995). In a survey of cool white dwarfs, Bergeron, Ruiz & Leggett (1997) obtain masses for 108 stars, of which only eight have masses $M \leq 0.4$ M$_\odot$, and none has a mass less than 0.25 M$_\odot$. A similar analysis of hotter white dwarfs (Bergeron et al. 1995) also found a scarcity of very low-mass stars. Bergeron et al. (1997) note that some of the stars with masses less than 0.4 M$_\odot$ are double degenerate binaries for which their analytical technique underestimates the mass by perhaps a factor of 2. Others appear to be truly single stars for which 'common envelope evolution is required to produce these low-mass degenerates because the Galaxy is not old enough to have produced them from single star evolution'. This inference may be a clue to the evolutionary origin of R CrB: is it the product of common envelope evolution?

One can, however, find empirical support for the low secondary mass from the binary 89 Her (Arellano Ferro 1984; Waters et al. 1993). This well known F2 supergiant has an infrared excess and a spectrum rich in 'sharp' emission lines, characteristics shared with R CrB. Waters et al. remark that, on the assumption that the primary has a mass of 0.6 M$_\odot$, the most probable mass for the secondary is 0.086 M$_\odot$ with an a priori 90 per cent probability that the mass of the secondary is less than 0.15 M$_\odot$. The orbital period of 89 Her is 288 d.

The He I broad lines presumably arise from the inner regions of the accretion disc. The cooler outer reaches of the disc may provide the lower excitation lines such as the Na I D lines. It is, perhaps, difficult in this scenario to understand why the widths of all broad lines are so similar. An alternative scenario such as a hot bipolar wind raises the question of what powers the wind, a question that is quite naturally answered in the context of an accretion disc around a compact object.

The binary model is testable. Since declines occur at random intervals, the broad emission lines detected during these declines

should be detected with both positive and negative velocity displacements relative to the systemic velocity. Studies of well-observed RCBs show that declines occur at random times and thus cannot be linked to particular orbital phases.

With fascination, we note that Alexander et al. (1972) report a velocity difference of about $66 \, \text{km s}^{-1}$ between the broad emission line 3889 Å and the mean velocity of RY Sgr. This difference was found on two occasions separated by about 200 d. This shift is of opposite sign to that we find for R CrB. Spite & Spite (1979) reported broad Na I D lines from RY Sgr redshifted by $37 \, \text{km s}^{-1}$ relative to Na I D and other sharp emission lines. At the 1993 minimum of RY Sgr Asplund (1995) found broad and sharp Na I D lines at the same radial velocity and remarked that 'this is contrary to the findings of Spite and Spite (1979) at the 1977 minimum'. Interestingly, the mean pulsational velocity also appears to change, suggesting the RY Sgr may be in orbit around an unseen companion. Alexander et al. (1972) show the mean velocity between -5 and $-10 \, \text{km s}^{-1}$ for 1969 and -10 and $-12 \, \text{km s}^{-1}$ for 1970, but measurements by Lawson et al. (1991) for 1988 give the mean velocity as $-21 \, \text{km s}^{-1}$. A range of at least 10 to $15 \, \text{km s}^{-1}$ is indicated over a long period. Thus there are data to suggest that RY Sgr may be a binary.

Other reports of He I lines include the detection of the 7065-Å line from S Aps (Goswami et al. 1997), where the line is essentially at the same velocity as the sharp emission lines but the broad Na I D lines are blueshifted by about $100 \, \text{km s}^{-1}$, implying that in this star the broad He I and broad Na I D lines have a different kinematical origin. The He I 3889-Å line was detected from U Aqr (Bond, Luck & Newman 1979), RS Tel (Feast & Glass 1973) and V CrA (Feast 1975). With the exception of S Aps, radial velocity measurements of the He I were not reported for these stars. In light of the fact that RCBs may have radial velocity amplitudes of $10-20 \, \text{km s}^{-1}$ from pulsations (Lawson & Cottrell 1997), it will require dedication to search for low-amplitude orbital velocity variations.

9.3 The veiled photospheric spectrum

When R CrB faded to below $V \simeq 12.5$, the character of the absorption-line spectrum changed, as noted in Section 8.2. Key changes of character are a redshift of the line core amounting to $10-20 \, \text{km s}^{-1}$, development of line broadening and extended red wings, and a 50 per cent decrease in equivalent width. These changes are qualitatively attributable to multiple scattering of the photospheric photons by circumstellar dust that is moving out from the star.

Van Blerkom & Van Blerkom (1978; see also Herbig 1969 and Kwok 1976) summarize Monte Carlo calculations of stellar light scattered off dust in a radially expanding, spherically symmetric and optically thick cloud. If the velocity of expansion is larger than the velocity width of a stellar line, multiple scattering via the attendant Doppler shifts broadens and redshifts the line. When the optically thick shell is also geometrically extended, the core of the emergent line profile is shifted by about the expansion velocity of the shell with a red wing extending to a few times the expansion velocity. Qualitatively, this prediction matches the profiles observed around minimum light with the velocity of expansion indicated to be about $25 \, \text{km s}^{-1}$. On the other hand, if the cloud is optically thick but geometrically thin, the line is only slightly redshifted and broadened. Van Blerkom & Van Blerkom give an eloquent explanation for the difference between profiles scattered

by geometrically thick and thin shells. Spherical symmetry is probably not required, but, to create a redshift, scattering clouds must be moving away from us. Indeed, the cloud causing the decline blocks the star, so that we see light from the far side scattered off the receding dust also on the far side. It is perhaps surprising that the apparent redshift of the scattered photospheric lines is so small in light of the expansion velocity suggested by the high-velocity Na I D components (next section). Clouds causing the decline must be between us and the star. Scattering within such clouds will impose no more than a very small Doppler shift on the scattered photons observed at Earth.

Transition of the normal photospheric profiles to the broadened shallow profiles occurs when the light scattered by the extended cloud and received at Earth is more intense than the light that penetrates the cloud causing the decline. If the extended cloud is a semi-permanent collection of clouds, and photospheric light reaches this shell from all parts of the star except that blocked by the cloud causing the observed decline, one expects that no decline of R CrB can be fainter than about $V \simeq 13.5$. It has been *assumed* previously (e.g. Whitney et al. 1992 for V854 Cen) that the light received during a long flat decline is not direct light absorbed by the new cloud, but light that is scattered by the other clouds. Our high-resolution spectra rather directly confirm this assumption in the case of R CrB – see also Rao & Lambert (1993) for confirmation for V854 Cen.

Scattering of starlight off dust will not change the equivalent width of an absorption line, but the broadened shifted lines seen at minimum light have a 50 per cent smaller equivalent width than their counterparts at other times. This could be an apparent change arising from very severe broadening and the loss of very extended wings owing to the limited signal-to-noise ratio of the spectra. Observations of the high-velocity absorption in the Na I D lines suggest that gas and, therefore, dust clouds can move at $200 \, \text{km s}^{-1}$. Scattering off such clouds will broaden lines by 200 to $300 \, \text{km s}^{-1}$ and result in very shallow, very broad lines which will be difficult to detect except at high signal-to-noise ratio. Thermal omission by the ensemble of distant dust clouds or the cloud causing the decline is unlikely to dilute the line spectrum.

Additional information could be gleaned from the wavelength dependence of the broadening and dilution of the absorption lines. Unfortunately, strong absorption lines at wavelengths shorter than those of the line sample considered here are low-excitation lines the absorption profile of which is obscured by overlying sharp emission. Clayton et al. (1997) find, from spectropolarimetry near minimum light, that red light is stellar light passing directly through the new dust cloud, but the blue light is scattered off an extended dusty region, a region which they identify as a bipolar flow off R CrB. This identification seems at odds with our scenario, but Clayton et al.'s observation refers to early 1996 April when our spectra show the absorption-line spectrum to be returning to its normal form. Regrettably, spectropolarimetry at minimum light has not been reported. However, as predicted by our model, the spectropolarimetric observations of V854 Cen at deep minimum do not show a change in position angle with wavelength (Whitney et al. 1992).

9.4 High-velocity ejection of gas

Broad absorption lines blueshifted by $100-200 \, \text{km s}^{-1}$ were seen in the Na I D lines during the recovery from minimum light. Their presence appears to be related to recovery from minimum light. In

the recovery from this decline, absorption was not seen in the Ca II H and K lines, implying that the ejecta were primarily neutral.

As argued in the previous section, direct light passing through the cloud causing the decline is a very minor contributor to the total light at magnitudes fainter than about 12.5 in the visual. Then, the gas associated with this cloud cannot be seen in absorption at minimum light. As the recovery progresses, the cloud thins and direct light transmitted through the cloud dominates the spectrum. This thinning is seen in the return of the photospheric absorption-line spectrum to its normal appearance. At this stage, sodium atoms in the associated gas are detectable in the spectrum. Acceleration of the gas is due to the radiation pressure on the grains and the momentum transfer by collisions between dust and gas. The velocity–time plot for the broad absorption lines (Fig. 25) suggests that acceleration began in early 1996 January when the star was at minimum light. The average acceleration is about $1 \, \mathrm{km \, s^{-1} \, d^{-1}}$. Perhaps fortuitously, this is close to the prediction illustrated by Fadeyev (1988 – see his fig. 4). An alternative view is that acceleration of the gas began earlier but was undetected because from 1995 mid-November to early 1996 April the contribution of light transmitted through the cloud to the total light was very slight. In this picture, the initial velocity of about $80 \, \mathrm{km \, s^{-1}}$ was attained over a longer period, extending from the onset of decline when dust first formed to the first appearance of the high-velocity Na I D absorption lines, an interval of about 100 d. In the initial stages, the gas at a low expansion velocity would be difficult to detect owing to blending with the strong sharp emission line. A series of spectra throughout a decline that led to a minimum in which the photosphere was directly observable throughout should betray the acceleration of the gas in the dust cloud responsible for the decline.

There has been an extended debate about the initial location of dust formation. Scenarios are usually characterized as 'near' and 'far' from the star. 'Near' and 'far' imply formation at about 2 and 20 stellar radii respectively. The acceleration is a potential clue to the location of the dust. Fadeyev's calculation refers to gas forming at about 20–25 stellar radii from the star. Approximate equality of observed and predicted accelerations implies that the dust and gas by early 1996 was at this distance. Our discovery of the photospheric trigger implies that dust condensed initially much closer to the star. All other things being equal, the radiative force on the grains scales inversely with the square of the distance from the star. Then, the acceleration of dust formed 'near' the star would be about 400 times greater than Fadeyev's prediction. Although the gas would have lagged behind the dust, one expects this acceleration of the dust to have led to an observable high velocity in resonance lines such as the Na I D and Ca II H and K lines. This was not observed. There are several ways to reduce the initial acceleration in the case that dust forms near the star. Not only does the radiative force increase with decreasing distance from the star, but so does the drag exerted by the gas because presumably the gas density in the cloud is higher near the star. In the initial phase of the decline when dust formation may be a continuing process, the dust-to-gas ratio is low and the drag on the grains necessarily higher than later in the decline. Additionally, dust formation near the star may result in a lower dust-to-gas ratio yet with adequate dust to initiate a decline. After the cloud becomes very optically thick, stellar photons will be multiply scattered and most likely absorbed such that the outer parts of the cloud experience a much reduced radiative force. In short, predictions about the initial acceleration of dust and gas formed near the star seem presently uncertain.

A change in the dust-to-gas ratio may occur as the cloud disperses and recovery to maximum light commences. Before dispersal of the cloud, sodium atoms and calcium ions may be largely condensed out on to the grains. As dispersal ensues, the equilibrium ratio of free atoms to atoms condensed on to grains necessarily shifts in favour of the former, as collisions between atoms/ions and grains decrease in frequency as the grains separate. Moreover, photons now penetrate the cloud and ejection of atoms from grains may proceed at an accelerated rate. This simple picture of a very optically thick cloud at minimum light accounts for the correlation between the appearance of the broad lines and the onset of the recovery phase.

9.5 Sharp emission lines: a circumbinary disc?

A variety of observational clues point to the location of the gas emitting the sharp emission lines. There are now strong indications that the lines are present at all times and, in sharp contrast to the transient lines, are not a product of the decline. Perhaps most significant is the fact that the lines, except for a drop in flux which occurs much later than the decline of the photospheric flux, are quite unaffected by the decline; their velocity, profile and degree of excitation and ionization are unchanged from onset to recovery. There is no evidence for interaction between the fresh dust cloud of the decline and the emitting region, from which we suppose that the late drop in flux is caused by occultation of a part of the emitting region and not by a quenching of the region.

Although observational material is limited, it appears that the results gathered here are representative of earlier declines of R CrB, and of declines of RY Sgr and V854 Cen. In particular, the sharp emission lines show a blueshift of up to about $10 \, \mathrm{km \, s^{-1}}$ relative to the stellar systemic velocity in all well-studied cases. This consistency and the absence of redshifts show that the asymmetry observed at Earth is quite unlikely to result from an asymmetric distribution of gas and dust around the star; an asymmetric distribution constructed without knowledge of the Earth's location must provide redshifts as well as blueshifts across a sample of RCBs.

We shall assume that the emitting gas is distributed symmetrically with respect to either R CrB, the putative companion, or the binary. The gas is sited about $20 \, R_*$ from the star in a thin layer. One possibility is that the gas is in a wind off R CrB, the companion, or the binary. The wind may be spherically or axially symmetric. Distribution of the permanent dust clouds affects the observed line flux and profile. We assume that the dust is distributed in either a spherical shell or a torus. A non-spherical or toroidal distribution of dust is suggested by the observational indications for a preferred plane for dust ejection. Since the dust shell radius $R_{\mathrm{dust}} \simeq 100 \, R_*$ is seemingly much larger than the binary separation ($6 \, R_*$?), the distinction between a shell centred on R CrB and one centred on its companion is immaterial. As viewed from Earth, the emission lines are blueshifted with respect to R CrB. Gas moving away from us must then be partially occulted by the star and/or seen through the dust in the extended dust cloud.

An expanding spherical shell with atoms everywhere within it moving outwards at a constant velocity v_{exp} provides a flat-topped emission profile for optically thin lines with a width $2v_{\mathrm{exp}}$ (Beals 1931) when the atomic emission coefficient has a profile much narrower than $2v_{\mathrm{exp}}$, and in other circumstances the observed

profile is a convolution of the flat-topped shell profile and that of the atomic emission coefficient. In the present case, the two profiles would seem to be of comparable width with $v_{exp} \simeq 10\,\text{km s}^{-1}$, so that their convolution produces a quasi-Gaussian profile. The observed blueshift of about $4\,\text{km s}^{-1}$ implies a relative reduction of intensity from the receding half of the emitting region.

If gas and dust are distributed in spherical shells of radii $R_{gas} \simeq 20\,R_*$ and $R_{dust} \simeq 100\,R_*$ respectively, the star occults a very small fraction of the receding gas: the fraction of gas shell that is occulted is $f = R_*^2/(4R_{sh}^2) \simeq 1/1600$ for $R_{sh} = 20\,R_*$. With the dust exterior to the gas, all regions of the gas shell are seen through the front of the dust shell, and approaching and receding regions are subject to the same extinction. In short, this geometry does not provide a blueshifted emission line of the magnitude observed. Of course, one may suppose the receding half of the gas shell to be thinner than the approaching half, but then the model is in conflict with the seemingly universal evidence for blueshifted sharp emission lines. A larger blueshift would result if the emitting gas were placed outside the dust shell (i.e. $R_{gas} > R_{dust}$), but this seems in conflict with estimates of the shell radii.

If the dust is confined to a torus, a line of sight grazing the lip of the torus provides a better view of the far side of the torus than the near side. If the gas inside the central hole of the torus is expanding radially, the net profile of the visible emitting gas will be redshifted not blueshifted. An inward flow of gas does not seem likely, and therefore we reject this model. If the gas is rotating and the gas on the far side from the observer's view is rotating towards us, a blueshift is expected. However, as the direction of rotation must differ from one RCB to another, this geometry would provide redshifts as often as blueshifts across a sample of RCBs. It does seem, however, that blueshifts are universal. We reject models with gas and dust in tori.

Our third possibility considers a spherically symmetric wind and a toroidal distribution of dust. If the inner radius of the dust torus is less than the inner radius of those portions of the wind emitting the sharp lines, the effect of the dust torus is to decrease the intensity of the redshifted relative to the blueshifted photons. The effect is a maximum for a line of sight perpendicular to the torus and vanishes for lines of sight in the plane of the torus. This geometry may be the simplest that meets the observational conditions, including the existence of a preferred plane for dust ejection. The line of sight to R CrB must obviously lie close to the preferred plane or declines would not be seen. Unfortunately, such a direction minimizes the blueshift. The allowed misalignment between plane and line of sight, and hence the magnitude of the blueshift, depends on the thickness of the torus, the inner shell radius of the torus, the degree of asymmetry in the wind, and the allowed ejection angle of dust near the star. Within this parameter space, it should be possible to generate the observed blueshift.

An outstanding question remains – how is gas distant from the star maintained at the physical conditions of the sharp line-emitting gas? Recall that the gas pressure is representative of that within a few pressure scaleheights of the photosphere. Is it possible that the sharp lines are emitted by compressed gas behind a shock that develops in the wind far from the star? Are the broad lines with their larger blueshifts related to the wind and its shock?

10   CONCLUDING REMARKS

Our study of the 1995–96 decline of R CrB has provided a wealth of new data on this fascinating episode. It is noteworthy that this decline was preceded by a long period during which the star was at or near maximum light, and therefore the spectroscopic phenomena are almost certainly attributable to the 1995–96 decline and not to the tailends of earlier declines. This situation may be sharply contrasted with the case of V854 Cen, which declines so frequently that spectroscopic changes resulting from one decline may overlap those of another.

Onset of the 1995–96 decline is strikingly correlated with a disturbance of the photospheric lines followed by the short-lived appearance of emission lines, including lines of high excitation which we refer to as transient lines and which seem to be the E1 lines according to Alexander et al.'s (1972) use of the terms E1 and E2. The sharp emission or E2 lines are present throughout the decline unchanged until the star is well into the minimum (m_V about 11 to 12). Their emitting region is remote from the star and is affected to a much lesser extent than the photosphere by the growth of the dust cloud responsible for the 1995 decline. Our new data are especially extensive for the broad permitted and forbidden lines. An intriguing result is the velocity shift of about $30\,\text{km s}^{-1}$ of the broad lines relative to the mean radial velocity of R CrB and to the sharp emission lines. If the shift is interpreted as orbital motion of the broad-line-emitting gas relative to R CrB, we argue that the secondary must be a low-mass object such as a white dwarf of about $0.2\,M$. We have noted the parallel with another enigmatic binary, 89 Her. If the broad He I lines are attributed to the accretion disc around the white dwarf, one is provided with a natural explanation for the heating and velocity of the emitting gas. We have noted that our proposal that R CrB is a previously unsuspected binary is testable with patience.

A key task for the future is to measure the broad-line radial velocity of R CrB at a series of deep declines, or, at maximum light, from the broad lines that are expected to be present in ultraviolet spectra obtainable with the *Hubble Space Telescope*. The C II 1335-Å multiplet is definitely present at maximum light in R CrB (Holm et al. 1987). Unfortunately, the *IUE* spectra from 1978–84 lack the resolution to assign the feature to the broad-line category. The fact that the 1335-Å flux of R CrB remained sensibly constant from maximum light into a decline at depth of about 4 mag is suggestive of an association with the broad-line region probed by our spectra. Unfortunately, the sharp lines in the 1995–96 decline also exhibited near-constant flux until the star had declined by more than 5 mag.

Optical and ultraviolet spectroscopy of other RCBs in decline and at maximum light is also of great importance. Optical observations in deep declines where broad emission lines may appear should be most valuable. Accurate velocities are needed for comparison with the systemic velocities which, in many cases, have yet to be determined to the desired accuracy. The C II 1335-Å multiplet is present in the spectrum of RY Sgr (Holm & Wu 1982; Clayton et al. 1999). This multiplet and C IV 1550 Å are present in the spectrum of V854 Cen at maximum light (Lawson et al. 1999); the photospheric contribution to the spectrum was undetectable on the available *IUE* spectra. The 1550-Å line is not present in the spectrum of RY Sgr at maximum light above the photospheric continuum as observed with the Space Telescope Imaging Spectrometer on the *Hubble Space Telescope* (*HST*/STIS) (Clayton et al. 1999). None of these observations of ultraviolet spectra provides the spectral resolution to distinguish broad from sharp emission lines. We would expect the C IV 1550-Å doublet to belong to the category of broad lines. The C II lines at 1335 and also at 2325 Å (Clayton et al. 1992, 1993) might be a mix of broad

and sharp lines.[6] In our picture, broad lines from an accretion disc around a secondary star cannot be affected by shocks in the photosphere of the primary. Observational evidence for profile variations of a broad line correlated with the pulsation of the primary would be incompatible with our attribution of these lines to an accretion disc. Lawson et al. (1999) and Clayton et al. (1992) found fading of flux in the suspected broad lines in UV region (e.g. Mg II, etc.) in some declines. It is possible on occasion, when the ejected dust cloud grows to large dimensions, that it could occult part of broad-emission-line region, resulting in some reduction in emission-line flux.

At issue is not simply whether R CrB has a companion. The presence of a companion may be a long-awaited clue to the evolutionary origins of these stars. The RCB family is largely homogeneous according to chemical composition. Asplund et al. (1999; see also Lambert & Rao 1994; Rao & Lambert 1996) show that a majority of known RCB stars have a composition quite similar to that of the eponym. A minority have strikingly different compositions. The similarity suggests that the majority may have a common origin. Then, if R CrB is a binary, one might expect the other majority members also to be binaries. One proposal for forming RCBs invokes a binary – the merger of a He white dwarf with a C–O white dwarf (Schönberner 1986, 1996; Iben, Tutukov & Yungelson 1996). The pair began as main-sequence stars and a common-envelope event began the merger process which may be completed by the emission of gravitational radiation. As considered to date, this process produces an RCB as a single star. This model is most unlikely to account for the wide binary that is conjectured here for R CrB; the merger process requires contact between the white dwarfs but the separation between R CrB and its companion in our model is about 10^5 times larger. Then a clear demonstration that R CrB is a binary will imply that either R CrB was formed by mass transfer across a wide binary or the companion is a relatively innocent bystander. The latter possibility will be difficult to sustain if it can be shown that binarity is common among the majority sample.

What is clearly needed from observers is a concerted *long-term* exploration of RCBs, both in decline and at maximum light. Ultraviolet spectroscopy should reveal broad lines even at maximum light. Observations of these lines repeated at intervals may reveal the orbital velocity variations of the secondary and its accretion disc. Spectroscopy of RCBs in deep declines should be pursued and velocity measurements made on the broad emission lines. These should eventually show the orbital velocity of the secondary. Precise and frequent observations of the RCB velocities may reveal the orbital velocity of the RCB primary, but this will be difficult as the pulsational amplitude may exceed the orbital amplitude in most cases. The ultimate goal is an important one: understanding the evolutionary origins of the most enigmatic of variable stars.

ACKNOWLEDGMENTS

REFERENCES

Alexander J. B., Andrews P. J., Catchpole R. M., Feast M. W., Lloyd Evans T., Menzies J. W., Wisse P. N. J., Wisse P., 1972, MNRAS, 158, 305
Aller L. H., 1984, Physics of Thermal Gaseous Nebulae. Reidel, Dordrecht
Arrellano Ferro A., 1984, PASP, 96, 641
Asplund M., 1995, A&A, 294, 763
Asplund M., Gustafsson B., Kiselman D., Eriksson K., 1997, A&A, 318, 521
Asplund M., Gustafsson B., Lambert D. L., Rao N. K., 1999, A&A, in press
Beals C. S., 1931, MNRAS, 91, 966
Bergeron P., Wesemael F., Lamontagne R., Fontaine G., Saffer R. A., Allard N. F., 1995, ApJ, 449, 258
Bergeron P., Ruiz M. T., Leggett S. K., 1997, ApJS, 108, 339
Bond H. E., Luck R. E., Newmann M. J., 1979, ApJ, 233, 205
Clayton G. C., 1996, PASP, 108, 225
Clayton G. C., Whitney B. A., Stanford S. A., Drilling J. S., Judge P. G., 1992, ApJ., 384, L19
Clayton G. C., Lawson W. A., Whitney B. A., Pollacco D. L., 1993, MNRAS, 264, L13
Clayton G. C., Lawson W. A., Cottrell P. L., Whitney B. A., Stanford S. A., de Ruyter F., 1994, ApJ, 432, 785
Clayton G. C., Whitney B. A., Meade M. R., Babler B., Bjorkman K. S., Nordsieck K. H., 1995, PASP, 107, 416
Clayton G. C., Bjorkman K. S., Nordsieck K. H., Zellner N. E. B., Schulte-Ladbeck R. E., 1997, ApJ, 476, 870
Clayton G. C., Ayres T. R., Lawson W. A., Drilling J. S., Woitke P., Asplund M., 1999, ApJ, 515, 351
Cottrell P. L., Lambert D. L., 1982, Observatory, 102, 149
Cottrell P. L., Lawson W. A., Buchhorn M., 1990, MNRAS, 244, 149
Danziger I. J., 1963, PhD thesis, Australian National University
Deutsch A. J., 1958, AJ, 63, 49
Espin T. E., 1890, MNRAS, 51, 12
Fadeyev Yu. A., 1986, in Hunger K., Schönberner D., Rao N. K., eds, Hydrogen Deficient Stars and Related Objects. Reidel, Dordrecht, p. 441
Fadeyev Yu. A., 1988, MNRAS, 233, 65
Feast M. W., 1975, in Sherwood V. E., Plaut L., eds, Variable Stars and Stellar Evolution. Reidel, Dordrecht, p. 129
Feast M. W., 1979, in Bateson F. M., Smak J., Ulrich I. M., eds, Changing Trends in Variable Star Research. Univ. Waikato, Hamilton, p. 246
Feast M. W., 1996, in Jeffery C. S., Heber U., eds, ASP Conf. Ser. Vol. 96, Hydrogen-Deficient Star. Astron. Soc. Pac., San Francisco, p. 3
Feast M. W., Glass I. S., 1973, MNRAS, 161, 293
Feast M. W., Carter B. S., Roberts G., Marang F., Catchpole R. M., 1997, MNRAS, 285, 317
Fernie J. D., 1989, PASP, 101, 166
Fernie J. D., 1991, PASP, 103, 1091
Fernie J. D., Lawson W. A., 1993, MNRAS, 265, 899
Fernie J. D., Seager S., 1994, PASP, 106, 1138
Fernie J. D., Sherwood V., DuPuy D. L., 1972, ApJ, 172, 383
Forrest W. J., Gillett F. C., Stein W. A., 1971, ApJ, 170, L29
Forrest W. J., Gillett F. C., Stein W. A., 1972, ApJ, 178, L129
Giridhar S., Lambert D. L., Gonzalez G., 1998, ApJ, 509, 366

---

[6] For V854 Cen observed at minimum light, Clayton et al. (1993) claimed that low-resolution *IUE* spectra showed splitting or doubling at a particular pulsational phase. Our examination of these *IUE* spectra in the final archive shows the lines to be single and unsplit, a conclusion also reached by Lawson et al. (1999).

Gorynya N. A., Rastorguev A. S., Samus N. N., 1992, Sov. Astron Lett., 18, 142

Goswami A., Rao N. K., Lambert D. L., Smith V. V., 1997, PASP, 109, 270

Herbig G. H., 1949, ApJ, 110, 143

Herbig G. H., 1968, Mem. Soc. R. Sci. Liège, 18, 353

Herbig G. H., 1969, Mem. Soc. R. Sci. Liège, 19, 13

Holm A. V., Wu C.-C., 1982, in Kondo Y., Mead J., Chapman R. D., eds, Advances in Ultraviolet Astronomy: Four Years of *IUE* Research. NASA CP-2238, 429

Holm A. V., Hecht J., Wu C.-C., Donn B., 1987, PASP, 99, 497

Iben I., Jr, Tutukov A. V., Yugelson L. R., 1996, in Jeffery C. S., Heber U., eds, ASP Conf. Ser. Vol. 96, Hydrogen Deficient Stars. Astron. Soc. Pac., San Francisco, p. 409

Joy A. H., 1926, ApJ, 63, 281

Joy A. H., 1954, ApJ, 1, 39

Keenan P. K., Greenstein J. L., 1963, Contrib. Perkins Obs., Ser. II, 13, 198

Kwok S., 1976, J. R. Astron. Soc. Can., 70, 49

Lambert D. L., Rao N. K., 1994, JA&A, 15, 47

Lambert D. L., Rao N. K., Giridhar S., 1990, JA&A, 11, 475

Lambert D. L., Heath J., Lemke M., Drake J. J., 1996, ApJS, 103, 183

Lawson W. A., 1986, in Hunger K., Schönberner D., Rao N. K., eds, Hydrogen Deficient Stars and Related Objects. Reidel, Dordrecht, p. 211

Lawson W. A., Cottrell P. L., 1997, MNRAS, 285, 266

Lawson W. A., Cottrell P. L., Clark M., 1991, MNRAS, 251, 687

Lawson W. A., Cottrell P. L., Gilmore A. C., Kilmartin P. M., 1992, MNRAS, 256, 339

Lawson W. A. et al., 1999, AJ, 117, 3007

Livio M., Warner B., 1984, Observatory, 104, 152

McCarthy J. K., Sandiford B. A., Boyd D., Booth J., 1993, PASP, 105, 881

Martin G. A., Fuhr J. R., Wiese W. L., 1988, J. Phys. Chem. Ref. Data, 17, No. 3

Mendoza C., 1983, in Flower D. R., ed., Planetary Nebulae. Reidel, Dordrecht, p. 43

Moore C. E., 1993, Tables of Spectra of Hydrogen, Carbon, Nitrogen, and Oxygen Atoms and Ions. CRC Press, Boca Raton

O'Keefe J. A., 1939, ApJ, 90, 294

Pandey G., Rao N. K., Lambert D. L., 1996, MNRAS, 282, 889

Payne-Gaposchkin C., 1963, ApJ, 138, 320

Pugach A. F., 1977, Inf. Bull. Variable Stars, 1277

Rao N. K., 1974, PhD thesis, University of California, Santa Cruz

Rao N. K., Lambert D. L., 1993, AJ, 105, 1915

Rao N. K., Lambert D. L., 1996, in Jeffery C. S., Heber U., eds, ASP Conf. Ser. 96, Hydrogen-Deficient Stars. Astron. Soc. Pac., San Francisco, p. 43

Rao N. K., Lambert D. L., 1997, MNRAS, 284, 489

Rao N. K., Nandy K., 1986, MNRAS, 222, 357

Raveendran A. V., Ashoka B. N., Rao N. K., 1986, in Hunger K., Schönberner D., Rao N. K., eds, Hydrogen Deficient Stars and Related Objects. Reidel, Dordrecht, p. 191

Reimers D., Cassabella A., 1985, ApJ, 297, 275

Risberg G., 1968, Ark. Fys., 37, 231

Schönberner D., 1986, in Hunger K., Schönberner D., Rao N. K., eds, Hydrogen Deficient Stars and Related Objects. Reidel, Dordrecht, p. 471

Schönberner D., 1996, in Jeffery C. S., Heber U., eds, ASP Conf. Ser. Vol. 96, Hydrogen-Deficient Stars. Astron. Soc. Pac., San Francisco, p. 433

Spite F., Spite M., 1979, A&A, 80, 61

Stanford S. A., Clayton G. C., Meade M. R., Nordsieck K. H., Whitney B. A., Murison M. A., Nook M. A., Anderson C. M., 1988, ApJ, 325, L9

Stecker D. W., 1973, AJ, 80, 451

Surendiranath R., Rangarajan K. E., Rao N. K., 1986, in Hunger K., Schönberner D., Rao N. K., eds, Hydrogen Deficient Stars and Related Objects. Reidel, Dordrecht, p. 199

Tull R. G., MacQueen P. J., Sneden C., Lambert D. L., 1995, PASP, 107, 251

Van Blerkom J., Van Blerkom D., 1978, ApJ, 225, 482

Vanture A. D., Wallerstein G., 1995, PASP, 107, 244

Viotti R., 1976, ApJ, 204, 293

Wamsteker W., 1981, A&A, 97, 329

Warner B., 1972, MNRAS, 159, 95

Warner B., 1995, Cataclysmic Variables. Cambridge Univ. Press, Cambridge

Waters L. B. F. M., Waelkens C., Mayor M., Trams N. R., 1993, A&A, 269, 242

Whitney B. A., Clayton G. C., Schulte-Ladbeck R. E., Meade M. R., 1992, AJ, 103, 1652

Woitke P., 1997, Thesis, Technical University Berlin

Woitke P., Goeres A., Sedlmayr E., 1996, A&A, 313, 217

This paper has been typeset from a TEX/LATEX file prepared by the author.